

RELATIONSHIP BETWEEN MAXILLARY ANTERIOR ALVEOLAR ARCH FORM AND  
TOOTH ROOT AXIS IN CLASS I OCCLUSION: A CONE BEAM COMPUTED  
TOMOGRAPHY STUDY



A Thesis Submitted in Partial Fulfillment of the Requirements  
for the Degree of Master of Science in Esthetic Restorative and Implant Dentistry

Common Course

Faculty of Dentistry

Chulalongkorn University

Academic Year 2018

Copyright of Chulalongkorn University

ความสัมพันธ์ระหว่างรูปแบบส่วนโค้งกระดูกงูในขากรรไกรบนส่วนหน้าและแกนรากฟันใน  
ผู้ป่วยที่มีการสบฟันปกติประเภทที่ 1: ประเมินโดยการถ่ายภาพรังสีส่วนตัดอาศัยคอมพิวเตอร์  
ชนิดโคนบีม



วิทยานิพนธ์นี้เป็นส่วนหนึ่งของการศึกษาตามหลักสูตรปริญญาวิทยาศาสตรมหาบัณฑิต  
สาขาวิชาทันตกรรมบูรณะเพื่อความสวยงามและทันตกรรมรากเทียม ไม่สังกัดภาควิชา/เทียบเท่า  
คณะทันตแพทยศาสตร์ จุฬาลงกรณ์มหาวิทยาลัย  
ปีการศึกษา 2561  
ลิขสิทธิ์ของจุฬาลงกรณ์มหาวิทยาลัย



สุวีรา เพทายบรรลือ : ความสัมพันธ์ระหว่างรูปแบบส่วนโค้งกระดูกเบ้าฟันในขากรรไกรบนส่วนหน้าและแกนรากฟันในผู้ป่วยที่มีการสบฟันปกติประเภทที่ 1: ประเมินโดยการถ่ายภาพรังสีส่วนตัดอาศัยคอมพิวเตอร์ชนิดโคนบีม. ( RELATIONSHIP BETWEEN MAXILLARY ANTERIOR ALVEOLAR ARCH FORM AND TOOTH ROOT AXIS IN CLASS I OCCLUSION: A CONE BEAM COMPUTED TOMOGRAPHY STUDY) อ.ที่ปรึกษาหลัก : รศ. ทพ. ดร.อาทิพันธุ์ พิมพ์ ขาวขำ, อ.ที่ปรึกษาร่วม : รศ. ทพ.ประเวศ เสรีเชษฐพงษ์

วัตถุประสงค์: เพื่อศึกษาความสัมพันธ์ของมุมระหว่างแกนรากฟันและแกนกระดูกเบ้าฟันต่อรูปแบบของส่วนโค้งกระดูกเบ้าฟันส่วนหน้าและการจำแนกประเภทตำแหน่งรากฟันในแนวแกนแบ่งซ้ายขวาในบริเวณขากรรไกรส่วนหน้าที่ต้องการความสวยงามโดยใช้ภาพรังสีส่วนตัดอาศัยคอมพิวเตอร์ชนิดโคนบีม

วิธีการศึกษา: คัดเลือกภาพรังสีส่วนตัดอาศัยคอมพิวเตอร์ชนิดโคนบีมตามเกณฑ์คัดเข้าและเกณฑ์คัดออกเพื่อนำมาจำแนกตามรูปแบบของส่วนโค้งกระดูกเบ้าฟันส่วนหน้า (Bulyalert et al. 2018) และจำแนกประเภทตำแหน่งรากฟันในแนวแกนแบ่งซ้ายขวา (Kan et al. 2011) จากนั้นวัดมุมระหว่างแกนรากฟันและแกนกระดูกเบ้าฟันในตำแหน่งกึ่งกลางของแนวแกนแบ่งซ้ายขวาของฟันแต่ละซี่ในภาพรังสีส่วนตัดอาศัยคอมพิวเตอร์ชนิดโคนบีม วิเคราะห์ความสัมพันธ์ของมุมระหว่างแกนรากฟันและแกนกระดูกเบ้าฟันต่อรูปแบบของส่วนโค้งกระดูกเบ้าฟันส่วนหน้าและการจำแนกประเภทตำแหน่งรากฟันในแนวแกนแบ่งซ้ายขวาโดยใช้การวิเคราะห์ความแปรปรวนทางเดียวและการวิเคราะห์การถดถอย

ผลการศึกษา: ภาพรังสีส่วนตัดอาศัยคอมพิวเตอร์ชนิดโคนบีมจำนวน 98 ภาพถูกใช้ในการประเมินประเภทตำแหน่งรากฟันในแนวแกนแบ่งซ้ายขวามีความสัมพันธ์ต่อมุมระหว่างแกนรากฟันและแกนกระดูกเบ้าฟันมากกว่ารูปแบบของส่วนโค้งกระดูกเบ้าฟันส่วนหน้า โดยการทำนายความสัมพันธ์ของมุมระหว่างแกนรากฟันและแกนกระดูกเบ้าฟันต่อทั้งรูปแบบของส่วนโค้งกระดูกเบ้าฟันส่วนหน้าและรูปแบบแนวแกนแบ่งซ้ายขวาสามารถทำได้ผ่านสมการแสดงความสัมพันธ์

สรุปผลการทดลอง: มุมระหว่างแกนรากฟันและแกนกระดูกเบ้าฟันมีความสัมพันธ์ต่อรูปแบบของส่วนโค้งกระดูกเบ้าฟันส่วนหน้าและประเภทตำแหน่งรากฟันในแนวแกนแบ่งซ้ายขวา ดังนั้นข้อมูลเหล่านี้สามารถใช้ประกอบการวางแผนในการทำรากฟันเทียมได้

สาขาวิชา	ทันตกรรมบูรณะเพื่อความสวยงาม และทันตกรรมรากเทียม	ลายมือชื่อ นิสิต .....
ปีการศึกษา	2561	ลายมือชื่อ อ.ที่ปรึกษาหลัก .....
		ลายมือชื่อ อ.ที่ปรึกษาร่วม .....

# # 5875833032 : MAJOR ESTHETIC RESTORATIVE AND IMPLANT DENTISTRY

KEYWORD: Alveolar Arch Form, Cone-Beam Computed Tomography, Root Angulation,  
Sagittal Root Position

Suweera Petaibunlue : RELATIONSHIP BETWEEN MAXILLARY ANTERIOR ALVEOLAR ARCH FORM AND TOOTH ROOT AXIS IN CLASS I OCCLUSION: A CONE BEAM COMPUTED TOMOGRAPHY STUDY. Advisor: Assoc. Prof. Atiphan Pimkhaokham, Ph.D.  
Co-advisor: Assoc. Prof. Pravej Serichetaphongsa

Purpose: This study determined the relationships of the angulation between tooth root axis and alveolar bone axis to the anterior alveolar (AA) arch forms and the sagittal root position (SRP) classification in anterior esthetic region using cone-beam computed tomography (CBCT) images.

Materials and Methods: CBCT images which met the inclusion and exclusion criteria were classified according to a novel classification of AA arch forms (Bulyalert 2018) and a SRP classification (Kan 2011). Then, the angulations of the root axis and the alveolar bone axis were measured using the mid-sagittal CBCT images of each tooth. The relationship of the angulations in each AA arch forms and the SRP classifications were evaluated using *one-way ANOVA* and linear regression model.

Results: 98 CBCT images were included in this study. The correlation of the angulations of the root axis and the alveolar bone axis to the SRP classification was greater than that to the classification of AA arch form. However, the relationship of the angulation of root axis and the alveolar bone axis to both the AA arch form classification and the SRP classification could be predicted.

Conclusion: The angulations of root axis and alveolar bone axis demonstrated the relationship to the classification of AA arch forms and the SRP classification. Therefore, this information could help implantologist in treatment planning.

Field of Study:	Esthetic Restorative and Implant Dentistry	Student's Signature .....
Academic Year:	2018	Advisor's Signature .....
		Co-advisor's Signature .....

## ACKNOWLEDGEMENTS

We thank Assoc. Prof. Pagaporn Pantuwadee Pisarnurakit and Asst. Prof. Dr. Vitara Pungpaong for statistical analysis assistance. The authors deny any conflicts of interest related to this study.

Suweera Petaibunlue



## TABLE OF CONTENTS

	Page
ABSTRACT (THAI).....	iii
ABSTRACT (ENGLISH).....	iv
ACKNOWLEDGEMENTS.....	v
TABLE OF CONTENTS.....	vi
LIST OF TABLES.....	viii
LIST OF FIGURES.....	x
CHAPTER I INTRODUCTION.....	1
1.1 Background and rationales.....	1
1.2 Research question.....	3
1.3 Research objectives.....	4
1.4 Hypothesis.....	4
1.5 Conceptual framework.....	4
1.6 Keywords.....	5
1.7 Expected benefit and application.....	5
1.8 Limitations of research.....	6
1.9 Research design.....	6
1.10 Ethical consideration.....	6
CHAPTER II.....	7
REVIEW OF LITERATURES.....	7
2.1 Implant.....	7
2.2 Alveolar bone.....	7

2.3 Arch forms .....	8
2.4 Alveolar arch forms .....	10
2.5 Tooth root position and angulation .....	14
2.6 Radiographic analysis.....	18
CHAPTER III MATERIALS AND METHODS .....	21
3.1 Materials.....	21
3.2 Methods .....	21
3.2.1 Image selection .....	22
3.2.2 Data collection .....	24
3.2.3 Examiner calibration.....	24
3.2.4 Anterior maxillary arch form measurement and classification.....	24
3.2.5 Sagittal root position (SRP) classification .....	30
3.2.6 Angulation evaluation.....	31
3.2.7 Data analysis .....	34
CHAPTER IV RESULTS .....	36
CHAPTER V DISCUSSION .....	45
REFERENCES .....	54
APPENDIX.....	61
VITA.....	76



## LIST OF TABLES

	Page
Table 1 Inclusion and exclusion criteria for image selection.....	23
Table 2 Definitions of arch form variables .....	26
Table 3 The characteristic, ranges of arch dimension and sample size of four groups of alveolar arch form.....	29
Table 4 Definitions of angulation landmarks.....	32
Table 5 Mean and standard deviation (SD) of sagittal angles between root axis and alveolar bone axis. ....	37
Table 6 Comparison of means and standard deviations of the sagittal angle of root axis and alveolar bone axis between the four groups of anterior alveolar arch form.	38
Table 7 Sagittal root position frequency distribution of the anterior maxillary incisors and first premolars in the alveolar bone. ....	40
Table 8 Angulation of the maxillary incisors and first premolars with reference to the alveolus according to the sagittal root position classification (14). ....	40
Table 9 Frequency distribution of anterior alveolar arch form and SRP in the alveolar bone of the anterior maxillary incisors and first premolars .....	42
Table 10 Linear regression analysis of the alveolar arch form and sagittal root position in relation to the sagittal root angulation between the tooth root axis and alveolar bone axis. <sup>a</sup> .....	44
Table 11 Data of the previous studies and the present report of the root angulation of the maxillary anterior teeth within the alveolar bone .....	46
Table 12 Data of the Kan's study and the present study of the frequency distribution of the root position of the anterior maxillary teeth in the alveolar bone	49

Table 13 Data of the previous study and the present study of the frequency distribution of the palatal root position of the anterior maxillary teeth in the alveolar bone .....	50
---	----



## LIST OF FIGURES

	Page
Figure 1 Conceptual framework of this study .....	5
Figure 2 Diagram of study design .....	21
Figure 3 Anterior maxillary arch measurement. Intermaxillary central incisor width, intercanine width, and interpremolar width are called aa', bb', and cc' line respectively. The shortest distances connecting the intercanine width and interpremolar width to the midpoint of aa' line are called intercanine depth (a <sub>m</sub> b <sub>m</sub> line) and interpremolar depth (a <sub>m</sub> c <sub>m</sub> line).....	27
Figure 4 The characteristics of alveolar arch form. Type1 (long narrow), type 2 (short medium), type 3 (long medium), and type 4 (long wide) were showed by the red, black, green, and purple curves respectively.....	28
Figure 5 The sagittal root position classification reported by Kan et al. (15). .....	31
Figure 6 Long axis of alveolar bone. Line A represented alveolar bone axis which was the line that bisecting the angle between the buccal line (Line 1) and the palatal line (Line 2). .....	33
Figure 7 Long axis of tooth root. Line B represented tooth root axis which was the line drawn from midpoint of the cervical line (Line3) to the root apex. ....	33
Figure 8 Diagram of the angulation between the alveolar bone axis and the tooth root axis. C° represented the angle between the alveolar bone axis (Line A) and the tooth root axis (Line B).....	34
Figure 9 Representative pictures of sagittal root position in our study. ....	39

# CHAPTER I

## INTRODUCTION

### 1.1 Background and rationales

The knowledge of dental implantation has gradually changed throughout the past fifty years. Presently, dental implant has become the standard treatment for dental reconstruction due to their high survival and success rate for both osseointegration and restoration. However, dental implant in the maxillary anterior esthetic zone has been a challenge for surgeons as a result of patients' esthetic expectations, functions and several risk factors which affect treatment outcomes, such as smile design, limited tooth space, supporting soft tissue, density and quantity of available bone at implant site etc.(1-5).

After tooth extraction, hard and soft tissue alterations can occur in both vertical and horizontal dimensions, especially on the facial aspect of the alveolar ridge (6, 7). From a biomechanical aspect, implants placed in the anterior maxilla are in the weakest section because they affect not only esthetic and phonetic outcomes, but also load distribution as well as loss of bone and soft tissue around implants (1). Thus, implants should be placed in appropriate three-dimensional position and angulation in the alveolar arch because they influenced type and position of prosthesis in a dental arch form.

Maxillary arch form and dental arch form were classified in many aspects in order to support the orthodontic treatment. Previous studies of maxillary arch form

or dental arch form were used the measurement from models (8-10) or human cadavers (11). This technique is not suitable for alveolar arch form measurement, thus the cone beam computed tomography (CBCT) has been recommended due to giving more accurate and reliable data, to analyze and classify the alveolar arch form at anterior maxilla (12).

Suk et al. (2013) were the first to report on the application of cone beam computed tomography (CBCT) by comparing the dental and basal arch forms in normal occlusion and Class III malocclusion cases (13). However, alveolar arch form gave more information for the implantologist in term of implant treatment planning and proper surgery. Using CBCT, Bulyalert and Pimkhaokham (2018) recently reported the classification of the alveolar arch form at the implant platform level in the maxillary anterior esthetic zone (14). This alveolar arch form classification would be helpful during the selection of implant size when determining the number of implants or implant axes and predicting bone augmentation, however, there is still no evidential support.

Root position is crucial for implant treatment planning in the anterior esthetic region, particularly in immediate implant therapy. Original root position in the alveolar bone explained the morphology of the post extraction site, which was able to predict future implant stability and bone perforation. Accordingly, Kan et al. categorized sagittal root position to aid implant treatment planning by classifying the relationship between the root position and its osseous housing (15).

The angulation of alveolar bone axis and long axis of whole tooth of anterior maxillary teeth were reported, it is mostly benefit for orthodontic treatment planning (16, 17). However, Bryant et al (1984) reported the mean angle between the long axis of crown and root of maxillary central incisor was 1.74 degree (18). This information could imply that the implant axis should be different from the whole tooth axis which were reported by Wang et al. (2014) and Zhang et al. (2015) (16, 17), since the implant should be placed mimic the natural and parallel to the tooth root axis. However, none of studies or reports has demonstrated the proper angulation of the natural tooth and the alveolar bone axis so far.

So far, none of studies related maxillary anterior alveolar arch form, sagittal root position, and angulation of dental root axis and alveolar bone axis, had been assessed. Thus, this study determined the relationship of alveolar arch forms, and tooth root axis in anterior maxillary region, using CBCT images.



## 1.2 Research question

Is there any relationship of the angulation between the tooth root axis and the alveolar bone axis in different alveolar arch form and different sagittal root position in maxillary esthetic zone?

### 1.3 Research objectives

The objective of this study is to analyze the relationship of the angulation between the tooth root axis and the alveolar bone axis, alveolar arch form, and sagittal root position in maxillary esthetic zone.

### 1.4 Hypothesis

**Null hypothesis:** There is no statistically significant difference in relationship of angulation between the tooth root axis and the alveolar bone axis in different alveolar arch form and different sagittal root position in maxillary esthetic zone.

**Alternative hypothesis:** There is statistically significant difference in relationship of angulation between the tooth root axis and the alveolar bone axis in different alveolar arch form and different sagittal root position in maxillary esthetic zone.

### 1.5 Conceptual framework

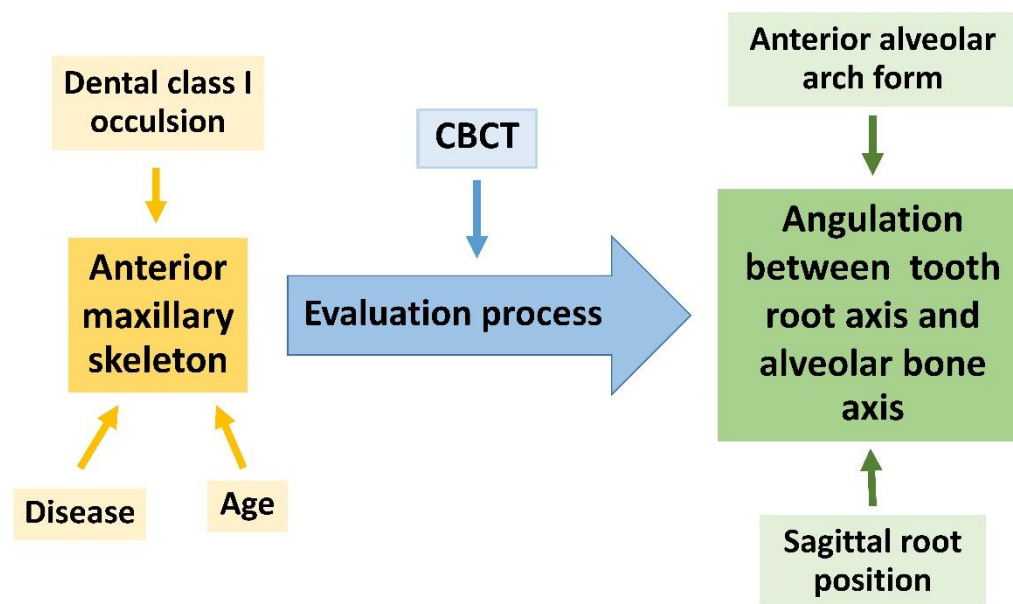


Figure 1 Conceptual framework of this study

#### 1.6 Keywords

Cone-Beam Computed Tomography; Tooth Root; Alveolar Process; Maxilla

#### 1.7 Expected benefit and application

The results of the research could demonstrate the influence of different types of maxillary anterior alveolar arch forms and different sagittal root position to angulation between alveolar bone axis and tooth root axis in anterior esthetic region. These results might provide the information of alveolar bone and tooth roots in anterior esthetic zone in order to help clinicians to place an implant in the ideal three-dimensional position with the same angulation of the original tooth root inside



the alveolar bone for achieving appropriate position for the restoration, good long-term functional and esthetic outcomes.

### **1.8 Limitations of research**

As there was no study about the relationship of anterior alveolar arch form, sagittal root position, and angulation between the tooth root axis and alveolar bone axis in anterior esthetic region. The sample size estimation of linear regression was 20 per group. From our database, the sample size of short medium arch was limited to 12. Although, according to the Multivariate Data Analysis of Hair (2006), the minimum ratio of observation was 5 per group, further studies are necessary to confirm the results(19).

### **1.9 Research design**

This study determined the relationship between alveolar arch forms, sagittal root position, and angulation of alveolar bone axis and tooth root axis in anterior maxillary region, including maxillary central incisors, lateral incisors, canines and first premolars, using cone-beam computed tomography.

### **1.10 Ethical consideration**

This study was conducted with the approval of the Ethics Committee of the Faculty of Dentistry, Chulalongkorn University, Bangkok, Thailand (HREC-DCU-P 2016-011).

## CHAPTER II

### REVIEW OF LITERATURES

#### 2.1 Implant

Nowadays, implant treatment has been a popular tooth replacement. The components of implant were including implant fixture which were placed and integrated in the alveolar bone as a prosthodontic foundation, implant abutment which connected to the implant fixture and restoration, might be constructed to accept screw- or cement- retained prosthetics. And restoration defined as material that replaced lost tooth structure or soft tissue (20).

Implant position needed to be considered in all three-dimensions and in relation to the adjacent teeth. The most challenging was the anterior maxilla where a malposition might jeopardize the treatment outcome. As a result, several authors recommended to place an implant no close than 1.5 mm to the adjacent root surface in the mesiodistal dimension. In the orofacial dimension, the implant shoulder was located 1 mm palatal to the point of the emergence at adjacent teeth as well as about 3 mm to the proposed gingival margin or 1 mm to cements enamel junction of the adjacent teeth (1, 21).

#### 2.2 Alveolar bone

Loss of teeth from alveolar bone caused lack of stimulating force to remaining bone and decreased in trabeculae and density of bone in the area with loss in external width and height of the bone volume. The residual ridge size was decreased

most rapidly in the first 6 months. After that, bone resorption activity of the residual ridge continued at a slower rate resulting in the large amounts of jaw structure (6, 7, 22). The change of alveolar bone might influence to the implant treatment planning.

In summary, alveolar bone affected the dentition. When tooth had lost, underlying alveolar bone changed overtime especially in the first year. Each alveolar area of maxilla and mandible were different depending on its anatomical structure, bone characteristics, bone quality and density, as well as curvature of arch.

### **2.3 Arch forms**

Arch forms were classified into 3 large categories; dental, bony and alveolar arch form. Many studies had been evaluated the characteristics of the dental arch forms (8, 9, 23, 24), the shapes of the bony arch form had been analyzed in few studies (13, 25, 26), whereas there were only few studies related to the classification of the alveolar arch form (10, 12). Dental arch form was defined as the curvature of dentition. The forms of dental arch were determined by several landmarks of teeth such as the most facial surface of the teeth, the midpoints of incisal edge and buccal cusp or central groove. Method of these studies included plaster models, photographs, CBCT images and statistical analysis (8, 13, 23, 27-29). Basal arch form was defined as the curvature of a band of soft tissue superior to the mucogingival junction or the WALA ridge (acronym for Will Andrews and Larry Andrews), but the soft tissue thickness among teeth varied, this might affect the positions of the WALA

point. The WALA band measured from dental casts and CBCT images (30, 31).

Alveolar arch form was defined as the curvature of alveolar bone that support the dentition. It was crucial because it was the region that support the future implant.

The studies related forms of the alveolar arch were performed using the models of Turkish patients by Uysal et al. (2005) (32, 33), and the CBCT images by Bulyalert et al. (2018) (13, 14).

The size and shape of the alveolar arches had considerable implications in diagnosis and treatment planning of implant therapy, affecting the dental esthetics, stability of the dentition, and space available in mesiodistal and labiopalatal dimensions of dentition. The forms of the alveolar arches were dictated by primary factors which were surrounding musculature, habits (thumb sucking), and metabolic activity within periodontal membrane and the secondary factors including postural position of head and eruption force of tooth. Variation in arch form occurred with normal growth and tended to increase the intermolar width during the changeover from the deciduous to the permanent dentition. The growth potential was difficult to predict in each patient. Arch width changes were different between male and female and the growth in width in the upper arch was more than the lower arch. The increase of intercanine and intermolar widths was seen between the ages of 3 to 13 years in both maxilla and mandible. Intercanine width remained stable or slightly increased in the maxilla and mandible after the permanent dentition erupted completely, that was 13 and 12 years of age respectively (29, 34-36).

However, arch form can be divided into 3 levels as mentioned before. In case of edentulous area, implant should be placed in proper position in the alveolar arch, so that the forms of alveolar arch are important.

#### **2.4 Alveolar arch forms**

The basal bone was defined as the maxillary or mandibular area that supported the alveolar process. Traditionally, the information of the form and size of basal arches as well as the relationship of teeth and basal arches, obtained from dental models, was evaluated to do treatment planning and predict prognosis after treatment. Afterwards, computer-based record keeping has been introduced. Digital photography and digital radiography have become more popular replacing analogue systems due to their adjustable image options and reasonable cost. Moreover, several studies found that digital study models could be a clinically acceptable alternative to conventional plaster models (37-39). Some studies evaluated the relationship of dental and basal arch forms on virtual models using the WALA ridge which was an acronym for Will Andrews and Larry Andrews who proposed a band of keratinized tissue immediately superior to the mucogingival junction of mandible, but soft tissue thickness which differed among teeth, affected the position of WALA point. A correlation between dental and basal width in canine and molar areas were highly significant (40-42). Recently, cone-beam computed tomography (CBCT) has been introduced and replaced traditional two-dimensional radiographs. Various studies had verified accuracy and reliability of CBCT images (43, 44).

Several studies had examined bony arch form in different methods. In 2007, Pietrokovski et al. evaluated arch shapes and angular determinations of completely edentulous dry human jaws with mature bone residual ridges. They reported that arches and ridges varied in size and shape. Edentulous maxillae were 65% ovoid, 25% triangular, and 10% irregular, whereas mandibular arches were 77% ovoid, 11% square, and 12% irregular. Angulations of maxillae and mandibles at the incisor, premolar and molar varied from 65° to 84° and 99° to 120° respectively (11).

According to the study of Sagat et al. in 2010, the three-dimensional finite element analysis method was done from models to evaluate stress concentration correspond to different alveolar arch shapes of the maxilla that coded as shortest ellipsoid shape and medium width, longest ellipsoid shape and narrow, U-shaped long and narrow, U-shaped short and wide and U-shaped medium length and medium width. And implant distribution models were coded on the basis of tooth number bilaterally as tooth 3,4,5; 2,3,4; 1,3,5; 2,4,5; 2,3,4,5. The implants supported a 12-unit bridge with the first molars region being the cantilever area. The results showed that the alveolar arch shape and implant distribution affected the maximum Von Mises stress values around peri-implant bone in both anterior and posterior regions. The stress values in the posterior region were higher than the anterior region, so that the cantilever area was critical for the posterior load. The use of 6 implants was not less advantageous than the use of 8 implants in longest ellipsoid shape and narrow, U-shaped long and narrow and shortest ellipsoid shape and medium width.

The relationship between the stress concentration and alveolar arch form demonstrated the good results when the implants were placed into lateral incisors, the first and the second premolars areas (10).

In 2013, Bayome et al. assessed the relationship of the mandibular dental and basal arches using CBCT and evaluated the correlation between dimensions of basal arch from CBCT and three-dimensional virtual models. The CBCT images were digitized facial axis points from right mandibular first molar to left mandibular first molar on the volume rendering view. And the root center digitized on a transverse section parallel to the occlusal plane at the level of the coronal 1/3 of the canine root, represented the basal arch dimension because it resembled the WALA points. In addition, some mandibular casts were scanned to the digital models to evaluate the dental and basal arch dimensions. The facial axis point and WALA point were also digitized. The study showed that correlations between dental and basal anterior and posterior arch widths were strong in normal occlusion, whereas no correlations were found between the arch depth measured from WALA points and root center points. The measurement of anterior and posterior basal widths on 3D models demonstrated a moderate correlation with those on CBCT. Therefore, root center points represented more practicable landmarks compared to WALA points in case of basal arch form evaluation (26).

The study of Suk et al. (2013) used the fourth degree polynomial equation to evaluate the relationship of the mandibular dental and basal arch forms. The facial

axis points and root center points were used as the anatomical reference points and identified from the right to the left first molar in the cone-beam computed tomography (CBCT) images. The intercanine and intermolar width, depth and width/depth ratio of both dental and basal arches were measured and calculated to generate the best fitting curve that represented the arch. For subjects with class III malocclusion, the dental and basal intercanine widths were larger than normal occlusion subjects. The distance between the facial axis points and the root center points significantly differed at each tooth except canines. And best-fitting curve of both groups had a significant difference in the anterior region. In addition, the dental and basal arch curves for each group were also different in arch shapes (13).

The recent article of Bulyalert et al. 2018 evaluated and classified arch form in anterior esthetic region at the level of implant shoulder using CBCT images. Root center points were identified at the level of 3 mm below cemento-enamel junction (CEJ) from the right to the left first premolars as the reference points. Four imaginary lines which were intercanine and interpremolar widths and depths were created. The values of intercanine and interpremolar width, depth and width/depth ratio were assessed. Anterior arch form classification was done using K-mean cluster analysis. The result of this study showed that the anterior arch form were divided into four types which were narrow high arch, medium short arch, medium high arch and wide high arch (14).



From previous reports (10, 11, 13, 14, 26), the classification of anterior alveolar arch form was essential for implant placement. In order to create successful long-term esthetic results, dental implants are necessary to place in a correct 3-dimensional position related to the different alveolar arch form. The position and angulation of tooth root might affect as well.

### **2.5 Tooth root position and angulation**

Previously, several studies had investigated the relationship between the roots of maxillary incisors and the surrounding alveolar structure with different reference landmarks (15-17, 45, 46). Each study attempted to evaluate dental alignment by observing tooth position and angulation. In 2011, Kim et al. investigated the relationship between maxillary incisor roots and alveolar structures in maxillae from Korean cadavers using microscopic computerized tomography (micro-CT). Labiopalatal cross-sectional images were used to measure the axial angle of the dental root (a line connecting the incisal edge and the root apex) to the alveolar bone (a line connecting the labiolingual midpoint of the alveolar and alveolar process) of the maxillary central and lateral incisors and canine. They found that the angle of the axis of the maxillary anterior tooth and the alveolar bone was greatest at the maxillary canine and smallest at the maxillary lateral incisor. The maxillary incisors and canine were positioned labially within the alveolar bone and their root axes were slightly tilted to the lingual aspect compared to the maxillary alveolar axes (45). It was similar to the study of Wang et al. in 2014, the sagittal angle

between the long axis of teeth and the long axis of the alveolar bone using the same reference landmarks as the study of Kim (2011) (45), were measured from CBCT images. They reported that the mean sagittal angles at the canines was greater than that at the incisors and premolars and it did not vary with age. Nearly 90% of the angle of maxillary incisors was  $\geq 10$  degree, but greater than 40% of canine was  $\geq 30$  degree (16). Whereas, Zhang et al. 2005 used cross-sectional CBCT images to evaluate the angulation formed by the long axis of the central incisor, lateral incisor and canine and the alveolus. The results showed that the maxillary anterior teeth were closer to the labial alveolar bone than the mandibular anterior teeth and the angulations of the maxillary anterior teeth were smaller from canine, lateral incisor and central incisor respectively (17).

According to the study of Lau et al. in 2011, the cone beam images were used to analyze the positions and angulations of the root of the central maxillary incisors with the alveolus in sagittal planes. The alveolar line which indicated the angulation of the alveolar process was formed by bisecting the palatal and buccal lines. The line of the tooth root was marked by the midpoint of a line drawn from the buccal enamel-dentin junction to its palatal part to the root apex. The position of tooth root was evaluated from the thickness of buccal and palatal bone at the mid-root level and the apical level. A classification was done according to the position and the angulation of the tooth root. The results demonstrated that the proportion of the central incisor positioning more buccally (type B), in midway (type M), and more

palatally (type P) were 78.8%, 19.4% and 1.8% respectively. Regarding the angulation of the alveolar process with the root axis, most of the central incisors (49.9%) were angulated toward the buccal side (type 2), 34.7% were classified that the root apices were positioned toward the buccal side passing anterior to point A (type 3) and 15.4% of root apices were angulated toward the palatal side or parallel to the alveolar process (type 1). The incidence of type B2 were found the most (38.2%), followed by type B3 (34.7%) and type M2 (11.7%). Type P2, P3, and M3 were not found (46).

Kan et al. 2011 used CBCT images to classify the relationship of the sagittal root positions of the maxillary anterior teeth to their osseous housing. Class I, II, III, IV were defined as the root was positioned against the labial cortical plate, was centered in the middle of the osseous housing without engaging at the apical third of the root, was positioned against the palatal cortical plate, and was engaging both the labial and palatal cortical plates at least two third of the root respectively. The results showed that class I, II, III, IV were found 81.1%, 6.5%, 0.7% and 11.7% respectively (15).

In 2014, Chung et al. evaluated and categorized the sagittal root relationship between the maxillary central incisors and alveolar bone housing into three groups, including buccal (Type B), medial (Type M), or palatal (Type P) using CBCT images. Moreover, a virtual rectangular frame representing the virtual dental implant, was performed using the software to observe the perforation of either the incisive canal

or labial cortical bone. They reported that the relationship between the root and the alveolar bone was not statistically significant difference between the sexes. 82% of the CBCT images showed no sign of contact between the rectangular frame and the incisive canal or labial cortex. A tapered body frame with a 3.5 mm apical diameter increased the success rate up to 98.8%. The location of the drilling access points met the crown on cingulum, incisal edge, and labial surface in 3.6%, 54.0%, and 42%, respectively (47).

Xu et al. (2016) determined CBCT images to classify the relationship of the sagittal root position of the maxillary central incisor within the respective alveolar bone as buccal, middle, and palatal. And the buccal type was further classified into subtype I, II, and III according to buccal bone thickness (48).

In 2017, Jung used the root position classification of Xu et al. (2016) to classify and analyzed the relationship of this classification, the buccal bone thickness, and the buccolingual angulation of the maxillary incisors using the CBCT images.

They found the root of the maxillary incisors were mostly located more buccally within the alveolar bone housing and only 0.5% of lateral incisors were positioned more palatally. The buccal subtype III showed the greatest angulation, while the middle type was the lowest angulation. Most of the maxillary incisors had a thin buccal bone wall and the maxillary lateral incisor showed a greater angulation than the maxillary central incisor (49).

According to the earlier studies, the position and angulation of tooth root were correlated with those of their alveolar bone. Therefore, tooth root position and angulation might relate to the future position of implant placement. A general evaluation of the facial structure should be start with smile analysis to create an optimal facial form. Several factors affected smile and esthetics, including lip display and contour, lip support, tooth size, shape, color, position and visibility, restoration, arrangement of dentition; especially the anterior teeth, and the gingival display (5). The existing teeth influenced both hard tissue configuration and soft tissue architecture. Space of edentulous area should be evaluated in three dimensions, including apicocoronal, faciolingual, and mesiodistal planes. Faciolingual inclination of both original and adjacent teeth should be considered as well. There were many techniques for 3D evaluation including; master models, fresh cadavers, virtual models or recently well-known DICOM data from cone beam computed tomography (CBCTs) (15-17, 45, 46).

## **2.6 Radiographic analysis**

Many imaging options were used to identify vital structures, determine the morphology of implant site, and assess the quality and quantity of bone before implant placement. Conventional radiographic techniques like periapical radiograph and panoramic radiography were the most commonly used, but they displayed only two-dimensions of mesio-distal width and apico-incisal height.

In the late 1990s, CBCT was initially introduced by Mozzo et al. (50). Due to the high-resolution images, CBCT had been used as a supplemental diagnostic technique for dental treatment in various fields of Dentistry, for example, Endodontics (51-54), Orthodontics (55-57), and Oral maxillofacial surgery (58, 59). In the field of implant dentistry, Cone beam computed tomography has become a common imaging technique that allowed the capture of information through a rotational movement of the radiation source and the detectors around the interesting region. It produced the three-dimension images for practitioners to visualize surrounding anatomical structure, identify pathology, and help plan prosthodontic and surgical treatment. For maxillofacial applications, CBCT technology offered the ability of reformatting the information of the axial slice into panoramic images, multiplanar cross-sectional images of interesting area and three dimensional volumetric reconstructions and using three-dimensional analysis with faster and easier data transformation including functional imaging and real time imaging for guiding interventional procedures (5, 60, 61). Currently, three-dimensional planning software was developed for not only treatment planning, but also to transfer to the surgical field through drilling templates that would help the surgeon to achieve a proper oral implant placement.

With the benefits of cone-beam computed tomography, it provided by offering safer and more accuracy outcomes for implant placement. Thus, the CBCT

data could be possibly used to determine the relationship between alveolar arch form, root position and angulation of alveolar bone and tooth root angulation.



## CHAPTER III

### MATERIALS AND METHODS

#### 3.1 Materials

1. CBCT images of 98 patients representing 4 types of anterior alveolar arch form were analyzed and selected from the computer record at the Faculty of Dentistry, Chulalongkorn University

2. Scanner (iCAT™, Imaging Science International, Hatfield, PA, USA) with a 170x130 mm. field of view

3. CBCT viewing software (*i-Dixel One Volume Viewer software Ver.1.5.0*; J. Morita Mfg. Corp., Kyoto, Japan)

#### 3.2 Methods

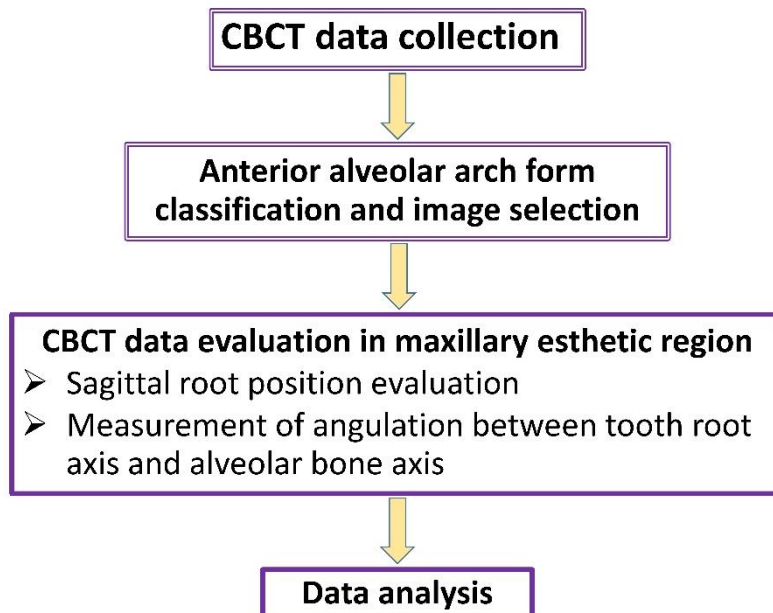


Figure 2 Diagram of study design



### 3.2.1 Image selection

CBCT images taken between January 2012 to December 2016 from the computer record at the esthetics and implant clinic of Chulalongkorn University which met the following criteria (Table 1), were used as the samples in this study.



**Table 1 Inclusion and exclusion criteria for image selection**

Inclusion criteria	Exclusion criteria
Images without any defects or artifacts	Images of patient with history of orthodontic treatment
Images present all maxillary anterior teeth and maxillary first premolar teeth	The presence of periodontal disease and bone
Patient's age at least 21 years old	The presence of root canal treatment
<p>All patients are Thai with class I occlusion</p> <ul style="list-style-type: none"> <li>- Class I molar and canine relationship</li> <li>- Arch length discrepancies of less than 2 mm.</li> <li>- Curve of spee of less than 2 mm.</li> <li>- Overbite approximates 20–30% of the height of the mandibular incisors.</li> <li>Overjet approximates 2-3 mm.</li> <li>Absence of tooth rotation and crowding</li> </ul>	The presence of tooth restoration
No radiographic evidence of surgical treatment	The presence of bone variation that affects the investigation
No radiographic evidence of infection, severe root resorption and trauma in anterior esthetic zone	

### 3.2.2 Data collection

All the images were acquired using CBCT scan (iCATTM. Imaging Sciences International, Hatfield, PA, USA) with a 170x130-mm field of view that resulted in 0.25 mm voxel size. The CBCT data were exported into digital imaging and communications in medicine (DICOM) files and imported into a CBCT viewing software (i-Dixel One Volume Viewer software Ver.1.5.0; J. Morita Mfg. Corp., Kyoto, Japan). All measurements were performed under 300 percent magnification by one examiner.

### 3.2.3 Examiner calibration

To ensure the reliability of the measurements obtained from the examiner, intra-examiner calibration was performed by measuring the variables, which are intercanine width, interpremolar width, intercanine depth, interpremolar depth, angle of the alveolar axis and tooth root axis of maxillary central incisors, lateral incisors, canines, and first premolars from CBCT images of 10 patients. The CBCT images were examined twice on separate days one month after the initial measurement. The results from the measurements were evaluated for intra-class correlation. The intraclass correlation coefficient (ICC) was performed using a 2-way mixed effects model to obtain a 95% level of confidence interval.

### 3.2.4 Anterior maxillary arch form measurement and classification

Anterior alveolar arch classification defined as the categories of curve of anterior maxillary alveolar arch from right to left maxillary first premolar teeth at the

implant related levels which was the level of 3 mm below cemento-enamel junction (CEJ) of right and left canines. The classification and the measurement of maxillary anterior alveolar arch form were briefly explained and cited from the study of Bulyalert et al. (14). To classify the anterior alveolar arch, the selected CBCT images were set horizontal plane parallel to the occlusal plane, anteroposterior plane parallel to median palatine suture, and vertical plane perpendicular to the horizontal and the anteroposterior planes. In axial view, the CBCT images were digitized at the level of 3 mm below cemento-enamel junction (CEJ) of the right and the left canines. Root center points of the right and the left maxillary central incisors (a and a'), the right and the left maxillary canines (b and b'), and the right and the left maxillary first premolars (c and c') were used as the reference points. The definitions of variables used for identify the arch form were shown in Table 2.

Table 2 Definitions of arch form variables

Variables	Definitions
Inter canine width	The distance between the root center points of the right and left maxillary canines on CBCT
Interpremolar width	The distance between the root center points of the right and left maxillary premolars on CBCT
Inter canine depth	The shortest distance from a line connecting the root center points of the right and left maxillary canines to the midpoint of the right and left maxillary central incisors on CBCT
Interpremolar depth	The shortest distance from line connecting the root center points of the right and left maxillary premolars to the midpoint of the right and left maxillary central incisors on CBCT

The measurements of variables were performed according to Table 2. The anterior alveolar arch form classification was evaluated using the three horizontal and the two vertical reference lines. The horizontal reference lines between root center points of the right and left maxillary central incisors, canines and first premolars were called as aa' line (Intermaxillary central incisor width), bb' line (intercanine width) and cc' line (interpremolar width) respectively. The vertical reference lines which were the shortest distances connecting the intercanine width

and interpremolar width to the midpoint of intermaxillary central incisor width (aa' line), were called intercanine depth ( $a_m b_m$  line) and interpremolar depth ( $a_m c_m$  line). The ratios of intercanine width/depth were calculated. All referent points and lines were presented in Figure 3.

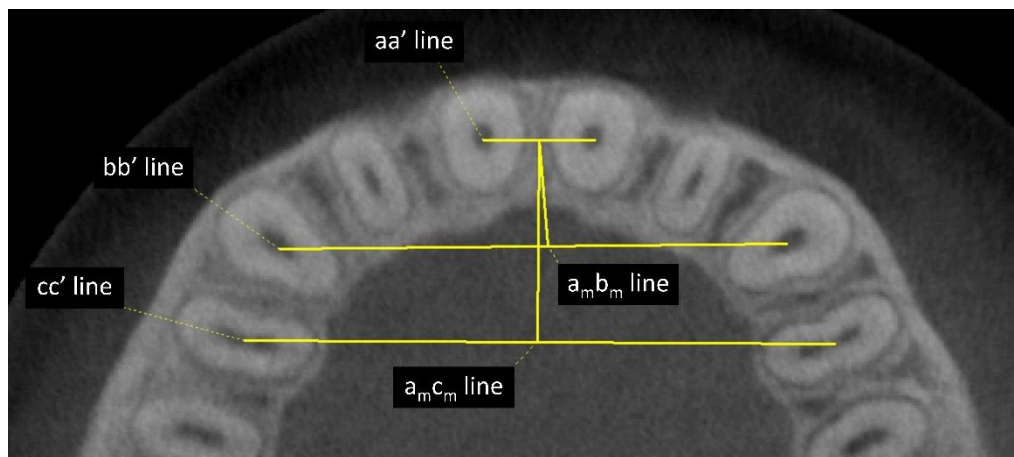


Figure 3 Anterior maxillary arch measurement. Intermaxillary central incisor width, intercanine width, and interpremolar width are called aa', bb', and cc' line respectively. The shortest distances connecting the intercanine width and interpremolar width to the midpoint of aa' line are called intercanine depth ( $a_m b_m$  line) and interpremolar depth ( $a_m c_m$  line).

Anterior alveolar arch curves were identified using the classification according to the study of Bulyalert et al. (14). They classified the anterior alveolar arch form into 4 groups including long narrow arch form, short medium arch form, long medium arch form, and long wide arch form. The classification method based on intercanine width, interpremolar width, intercanine depth, interpremolar depth and intercanine

width/depth ratio. The characteristic, ranges of arch dimension and sample size of each arch form were presented in Figure 4 and Table 3.

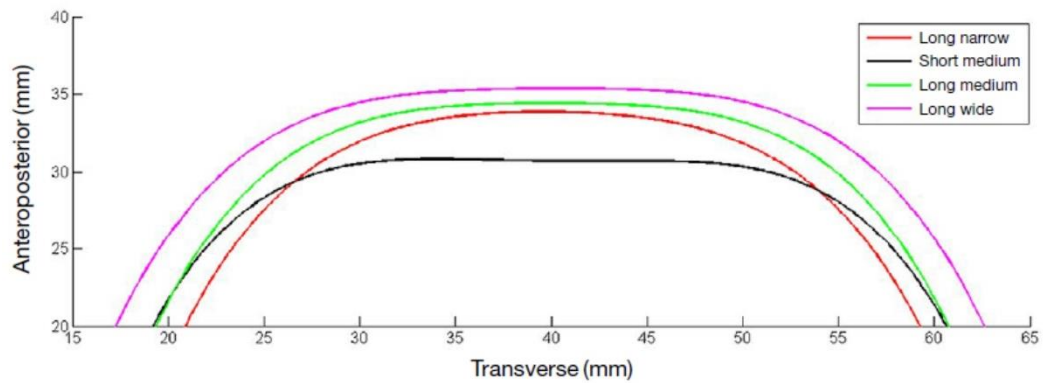


Figure 4 The characteristics of alveolar arch form. Type1 (long narrow), type 2 (short medium), type 3 (long medium), and type 4 (long wide) were showed by the red, black, green, and purple curves respectively.

Table 3 The characteristic, ranges of arch dimension and sample size of four groups of alveolar arch form

Group of arch form	Arch dimension	Mean (mm)	SD	Range of arch dimension
Long narrow arch (n=30)	Inter canine width (bb' line)	29.66	1.32	29.18-30.13
	Inter premolar width (cc' line)	36.01	1.39	35.51-36.51
	Inter canine depth (b <sub>m</sub> )	5.57	0.90	5.25-5.89
	Inter premolar depth (c <sub>m</sub> )	11.16	1.38	10.66-11.65
	Inter canine width/depth (bb'/b <sub>m</sub> )	5.45	0.85	5.15-5.76
Short medium arch (n=30)	Inter canine width (bb' line)	31.83	1.56	31.05-32.60
	Inter premolar width (cc' line)	38.96	1.41	38.26-39.67
	Inter canine depth (b <sub>m</sub> )	3.05	0.52	2.79-3.31
	Inter premolar depth (c <sub>m</sub> )	8.45	1.10	7.90-9.00
	Inter canine width/depth (bb'/b <sub>m</sub> )	10.70	1.70	9.85-11.54
Long medium arch (n=30)	Inter canine width (bb' line)	32.26	1.02	31.91-32.60
	Inter premolar width (cc' line)	38.75	0.84	38.46-39.03
	Inter canine depth (b <sub>m</sub> )	5.43	1.07	5.07-5.79
	Inter premolar depth (c <sub>m</sub> )	11.30	1.49	10.79-11.80
	Inter canine width/depth (bb'/b <sub>m</sub> )	6.14	1.07	5.78-6.30



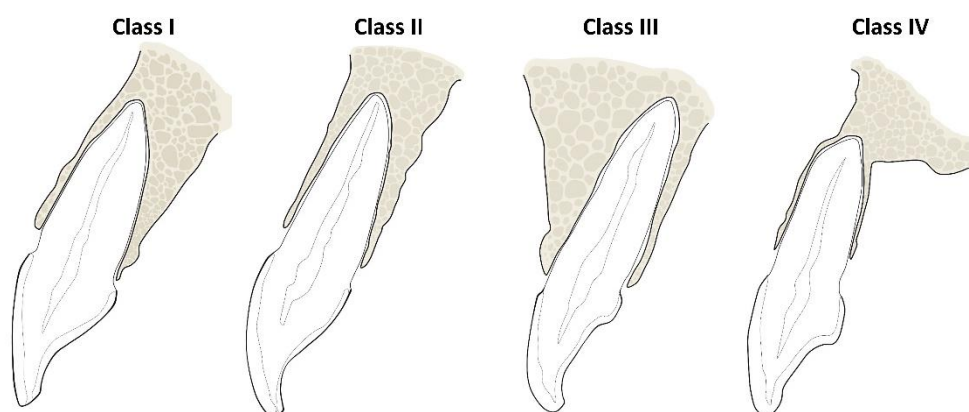
<b>Long wide arch (n=30)</b>	Inter canine width (bb' line)	35.01	1.26	34.51-35.51
	Inter premolar width (cc' line)	41.74	1.41	41.18-42.30
	Inter canine depth (bm)	5.28	0.96	4.90-5.66
	Inter premolar depth (cm)	11.35	1.42	10.79-11.91
	Inter canine width/depth (bb'/bm)	6.38	1.14	6.38-7.28

### 3.2.5 Sagittal root position (SRP) classification

The classification of SRP was defined based on the type of dental root position of the maxillary central incisors, lateral incisors, canine, and first premolars in their respective alveolar bone housing. Each tooth root image was classified according to the classification reported by Kan et al. (15) which divided tooth root position within its bone into four Classes, including class I, II, III, and IV as detailed in Figure 4. In Figure 4, class I includes the root was engaged with the buccal cortical bone, class II in which the root was in the middle of the alveolar bone housing and without engaging either the buccal or the palatal bone at the apical third of the root, meanwhile class III was

where the root was engaged with the palatal cortical bone, and finally class IV that was engaged to either the buccal or the palatal cortical bone.

Figure 5 The sagittal root position classification reported by Kan et al. (15).



### 3.2.6 Angulation evaluation

The angulation of alveolar bone axis and tooth root axis defined as the angle between alveolar bone axis and tooth root axis of maxillary central and lateral incisors, maxillary canine and maxillary first premolar teeth. To measure the angulation of alveolar bone axis and tooth root axis, the labio-lingual cross-section in the middle of mesio-distal dimension of the tooth was observed through the CBCT images. Landmarks were identified and marked before the measurement would be performed. The definitions of landmarks used for identify the angulation were shown in Table 4.

Table 4 Definitions of angulation landmarks

Landmarks	Definitions
<b>Buccal line</b>	The best fit line to the outer surface of buccal plate which contacted the buccal alveolar surface at the level of 3 mm below cemento-enamel junction (CEJ)
<b>Palatal line</b>	The best fit line to the outer surface of palatal plate which contacted the palatal alveolar surface at the level of 3 mm below cemento-enamel junction (CEJ)
<b>Cervical line</b>	The line drawn from the buccal to palatal aspects of the cemento-enamel junction (CEJ)

The measurement of alveolar bone axis was performed by drawing the buccal line (Line 1) and palatal line (Line 2). The alveolar line (Line A) was marked by bisecting angle between the buccal line (Line 1) and the palatal line (Line 2). The alveolar line represented the long axis of the alveolar bone in sagittal view (Figure 5). While, the measurement of tooth root axis (Line B) was marked by connecting line from midpoint of the cervical line (Line 3) to the root apex (Figure 6). The angle ( $C^\circ$ ) between the long axis of alveolar process (Line A) and the long axis of tooth root (Line B) were performed and measured using the computer software (*i-Dixel One Volume Viewer software* Ver.1.5.0; J. Morita Mfg. Corp., Kyoto, Japan). The measurements were shown in Figure 7.

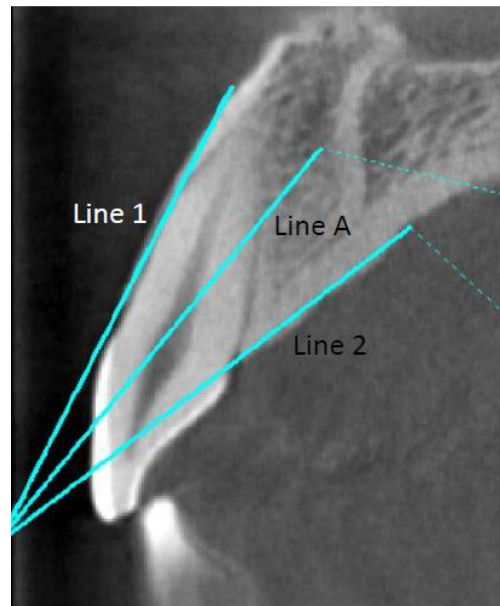


Figure 6 Long axis of alveolar bone. Line A represented alveolar bone axis which was the line that bisecting the angle between the buccal line (Line 1) and the palatal line (Line 2).

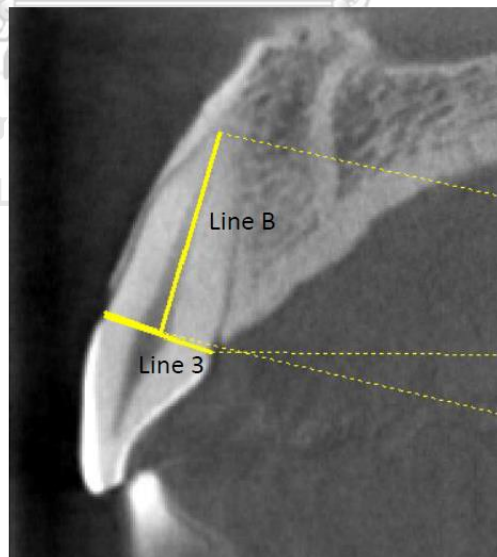


Figure 7 Long axis of tooth root. Line B represented tooth root axis which was the line drawn from midpoint of the cervical line (Line3) to the root apex.

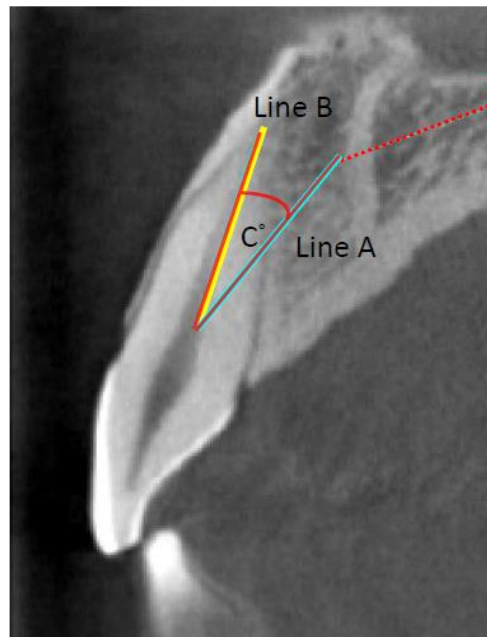


Figure 8 Diagram of the angulation between the alveolar bone axis and the tooth root axis.  $C^\circ$  represented the angle between the alveolar bone axis (Line A) and the tooth root axis (Line B).

The angulations between the alveolar bone axis and the tooth root axis of maxillary central incisor, maxillary lateral incisor, maxillary canine and maxillary first premolar were determined.

### 3.2.7 Data analysis

Each CBCT image was evaluated the classification of anterior alveolar arch, sagittal root position, and the angulation of the tooth root axis and the alveolar bone axis. The mean and standard deviation of the angulation between the tooth root axis

and the alveolar bone axis was calculated according to the different types of the AA arch forms and different sagittal root position. The data was analyzed using statistical software (IBM SPSS Statistics 22, IBM Corp., Armonk, NY, USA). The normality of the data was determined using the Shapiro-Wilk test. A comparative analysis with an independent T-Test and Pearson Product Moment *Correlation* was applied between the right and left sides of the alveolar arch form. Descriptive statistics were presented as means with standard deviations, frequencies, and percentages. *An analysis of variance (ANOVA)* with the Scheffe post-hoc test was performed to compare the angulation of the root axis and the alveolar bone axis of the maxillary incisors, and maxillary first premolars of the types of alveolar arch forms and the sagittal root position. The Tukey post-hoc test was used to compare the sagittal angulation of individual teeth. The influence of anterior alveolar arch forms and sagittal root position on the angulation between the root axis and the alveolar bone axis were studied through linear regression models.  $p$ -values  $< 0.05$  were judged as statistically significant differences

## CHAPTER IV

### RESULTS

In total, CBCT images from 98 patients matched the inclusion criteria for this study. The 196 CBCT images of the left and right maxillary central incisors, lateral incisors, canines and first premolars were evaluated. The mean sagittal angles between the root axis and the respective alveolar bone axis of each tooth are shown in Table 5. The mean sagittal angulation between the alveolar bone axis and the tooth root axis of maxillary central incisor was the largest angle and showed statistically significant greater than the others. There was no significant difference in the sagittal angulation of the alveolar bone axis and the tooth root axis between the right and left sides. However, a moderate level of correlation was found between the right and the left sides ( $r= 0.657$ ;  $p< 0.001$ ).

Table 5 Mean and standard deviation (SD) of sagittal angles between root axis and alveolar bone axis.

Tooth	Angle (degrees)	Range
	mean $\pm$ SD	(degrees)
Maxillary central incisor (n =196)	16.59 $\pm$ 5.97 <sup>A</sup>	1.10 – 33.12
Maxillary lateral incisor (n =196)	13.89 $\pm$ 6.12 <sup>B</sup>	0.67 – 32.41
Maxillary canine (n =196)	14.93 $\pm$ 6.02 <sup>B</sup>	-0.61 – 35.23
Maxillary first premolar (n =196)	13.38 $\pm$ 6.46 <sup>B</sup>	1.01 – 30.64

\*The sagittal angulation of each tooth is given in degrees; measurements are given as mean and standard deviation.

\*\*The same superscript capital letters indicate the absence of significant differences in sagittal angulation ( $p > 0.05$ ).

The classification results of the anterior alveolar arch form show that among the CBCT images there were 30 long narrow arches, 12 short medium arches, 30 long medium arches, and 26 long wide arches. The overall mean sagittal angulation of the root axis and alveolar bone axis in the short medium arch was significantly lower than that of both the long medium arch and the long wide arch. The sagittal angulation between the alveolar bone axis and root axis of the short medium arch was considered to be less significant difference than that of the long medium arch at the maxillary central incisor and canine. In addition, the sagittal angulation between



the alveolar bone axis and root axis of the maxillary central incisor of the long wide arch was statistically greater than that of the short medium arch (Table 6).

**Table 6 Comparison of means and standard deviations of the sagittal angle of root axis and alveolar bone axis between the four groups of anterior alveolar arch form.**

Arch form Tooth	Long narrow (n=60)	Short medium (n=24)	Long medium (n=60)	Long wide (n=52)
Central incisor	15.34 ± 5.88 <sup>A,B,C,D</sup>	13.49 ± 4.93 <sup>A</sup>	18.01 ± 5.19 <sup>B,D</sup>	17.81 ± 6.64 <sup>C,D</sup>
Lateral incisor	13.40 ± 6.35	11.24 ± 6.62	14.78 ± 5.75	14.66 ± 5.79
Canine	15.06 ± 6.79 <sup>A,B,C</sup>	11.57 ± 4.42 <sup>B</sup>	16.10 ± 5.99 <sup>C</sup>	14.99 ± 5.29 <sup>A,B,C</sup>
First premolar	12.35 ± 5.97	13.60 ± 6.28	13.05 ± 6.46	14.86 ± 6.98
Overall	14.04 ± 6.34 <sup>A,B,C,D</sup>	12.48 ± 5.65 <sup>A</sup>	15.09 ± 6.37 <sup>B,D</sup>	15.58 ± 6.30 <sup>C,D</sup>

\*Sagittal angulation of each tooth in different arch is given in degrees; measurements are given as mean standard deviation.

\*\*The same superscript capital letters indicate the absence of significant differences in sagittal angulation for each horizontal row ( $p > 0.05$ ).

The SRP were categorized according to Kan et al. (14). Most of the root of maxillary incisors and maxillary first premolars were positioned buccally within the

alveolar bone (Class I). Meanwhile, the sagittal root position which was engaging with the palatal cortical bone (Class III) was not found (Figure 8). The number (percentage) of sagittal root positions for Class I, II, III, and IV groups are shown in Table 7.

Statistically significant differences in the overall mean angles between the tooth root axis and alveolar bone axis were found between the Class groups I, II, and IV ( $p < 0.05$ ).

For the Class I sagittal root position, the mean angulation of the maxillary central incisor was the largest angle and significantly greater than the others.

However, for the Class II and IV sagittal root positions, significant differences between the mean root-to-bone angulations of the maxillary incisors and the first premolar were not found (Table 8).

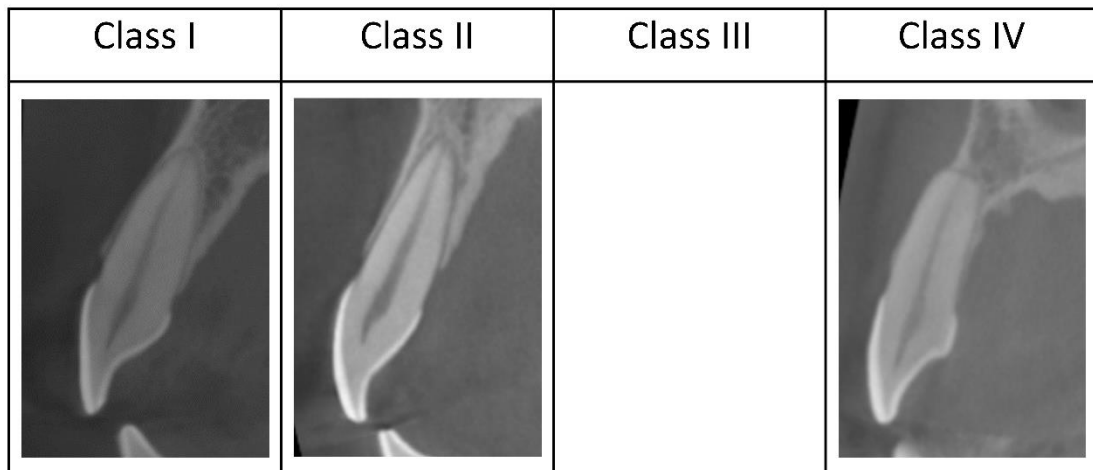


Figure 9 Representative pictures of sagittal root position in our study.

Table 7 Sagittal root position frequency distribution of the anterior maxillary incisors and first premolars in the alveolar bone.

Sagittal root position	Overall n (%)	Central incisor n (%)	Lateral incisor n (%)	Canine n (%)	First premolar n (%)
Class I	667 (85.10%)	156 (79.60%)	165 (84.20%)	194 (99.00%)	152 (77.60%)
Class II	82 (10.50%)	40 (20.40%)	10 (5.10%)	1 (0.50%)	31 (15.80%)
Class III	-	-	-	-	-
Class IV	35 (4.50%)	-	21 (10.70%)	1 (0.50%)	13 (6.60%)
Total	784	196	196	196	196

Table 8 Angulation of the maxillary incisors and first premolars with reference to the alveolus according to the sagittal root position classification (14).

SRP Tooth	Class I (degree)	Class II (degree)	Class III (degree)	Class IV (degree)
Central incisor	17.27 ± 5.60 <sup>A</sup>	13.91 ± 6.66	-	-
Lateral incisor	15.11 ± 5.62 <sup>B,C</sup>	11.42 ± 4.62	-	5.49 ± 2.69
Canine	14.99 ± 6.02 <sup>B,D</sup>	8.63 ± 0	-	9.84 ± 0
First premolar	14.09 ± 6.14 <sup>B,E</sup>	12.43 ± 7.61	-	7.37 ± 3.26
Overall	15.35 ± 5.96 <sup>*</sup>	12.98 ± 6.80 <sup>§</sup>	-	6.31 ± 3.04 <sup>†</sup>

\*Angulation of the maxillary incisors and first premolars are given in degrees; measurements are given as mean and standard deviation.

\*\*The same superscript capital letters indicate the absence of significant differences in angulation for each column ( $p > 0.05$ ).

\*\*\*The same symbols indicate the absence of significant differences in angulation for each horizontal row ( $p > 0.05$ ).

The SRP frequencies of each different anterior alveolar arch form of the maxillary central incisor to the maxillary first premolar are shown in Table 9. The SRP of the maxillary central incisor in every arch form were found only in classes I and II. More than 98% of the maxillary canines were classified as SRP Class I, whereas most of the maxillary first premolars were categorized as SRP class I, followed by classes II and IV, respectively.



**Table 9 Frequency distribution of anterior alveolar arch form and SRP in the alveolar bone of the anterior maxillary incisors and first premolars**

Arch form Tooth	Long narrow arch (n=30)				Short medium arch (n=12)				Long medium arch (n=30)				Long wide arch (n=26)			
	Class I n (%)	Class II n (%)	Class III n (%)	Class IV n (%)	Class I n (%)	Class II n (%)	Class III n (%)	Class IV n (%)	Class I n (%)	Class II n (%)	Class III n (%)	Class IV n (%)	Class I n (%)	Class II n (%)	Class III n (%)	Class IV n (%)
Maxillary central incisor	43 (71.7%)	17 (28.3%)	-	-	20 (83.3%)	4 (16.7%)	-	-	51 (85.0%)	9 (15.0%)	-	-	42 (80.8%)	10 (19.2%)	-	-
Maxillary lateral incisor	47 (78.3%)	6 (10.0%)	-	7 (11.7%)	18 (75.0%)	-	-	6 (25.0%)	52 (86.7%)	3 (5.0%)	-	5 (8.3%)	48 (92.3%)	1 (1.9%)	-	3 (5.8%)
Maxillary canine	60 (100%)	-	-	-	24 (100%)	-	-	-	59 (98.3%)	-	-	1 (1.7%)	51 (98.1%)	1 (1.9%)	-	-
Maxillary first premolar	45 (75%)	10 (16.7%)	-	5 (8.3%)	22 (91.7%)	2 (8.3%)	-	-	41 (68.3%)	12 (20.0%)	-	7 (11.7%)	44 (84.6%)	7 (13.5%)	-	1 (1.9%)

As shown in Table 10, the correlation between the alveolar arch form and SRP classification to the angle of root axis and alveolar bone axis were 2.5% and 9.5%, respectively. However, the anterior alveolar arch form together with the sagittal root position related to the angulation of the root axis and alveolar bone axis by approximately 11.7%. Even if, the angulation of root axis and the alveolar bone axis was influenced by the anterior alveolar arch form and the sagittal root position, the interaction between the anterior alveolar arch form and the sagittal root position was not found. Thus, the relationship between both the alveolar arch form and the sagittal root position with the angle of root axis and the alveolar bone axis followed the equation:

$$\text{Angle} = 7.101 - 1.161 \text{ long narrow arch} - 2.787 \text{ short medium arch} + 0.239 \text{ Long medium arch} + 8.867 \text{ SRP}_1 + 6.482 \text{ SRP}_2$$

Table 10 Linear regression analysis of the alveolar arch form and sagittal root position in relation to the sagittal root angulation between the tooth root axis and alveolar bone axis.<sup>a</sup>

	Alveolar arch form		Sagittal root position		Alveolar arch form* sagittal root position	
	B	p-value	B	p-value	B	p-value
(Constant)	15.579	<0.001	6.314	<0.001	7.101	<0.001
Long narrow	-1.544	0.009			-1.161	0.038
Short medium	-3.102	<0.001			-2.787	<0.001
Long medium	-0.091	0.876			0.239	0.669
SRP Class I			9.036	<0.001	8.867	<0.001
SRP Class II			6.668	<0.001	6.482	<0.001
SRP Class III			-	-	-	-
R	0.170		0.312		0.350	
Adjusted R Square	0.025		0.095		0.117	
F-value	7.777		42.138		21.773	
p-value	<0.001		<0.001		<0.001	

a. Dependent Variable: Angle.

b. Predictors: (Constant), long narrow, short medium, long medium, SRP Class I, SRP Class II, SRP Class III.

## CHAPTER V DISCUSSION

Our study determined the anterior alveolar arch form, the sagittal root position, and the angulation between the tooth root axis and the alveolar bone axis on the CBCT images. Previous studies paid attention to the dental and basal arches in order to focus on orthodontic treatment (13, 26, 62). For implant dentistry, only the alveolar arches were considered during implant treatment planning. The classification reported by Bulyalert et al. (2018) was the first to categorize the anterior alveolar arch form at the implant platform level utilizing CBCT imaging technique (14). Several studies investigated and classified the root position of maxillary anterior teeth in the alveolar bone using CBCT images (15, 46-48). In addition, some authors had interested in the sagittal root angulation of the maxillary teeth in the anterior esthetic zone. Therefore, this study reported the sagittal root angulation within the respective alveolar bone influencing by the anterior alveolar arch form and the sagittal root position.

To establish an ideal implant position, the angulation of implant is a significant factor for implant treatment planning. If implant could place in the alveolar bone at the same angulation as the original tooth root, the future prosthetic crown would align similar to adjacent teeth and a stock straight implant abutment would be needed (16, 46). The results demonstrated that sagittal angles between root axis and alveolar bone axis of the maxillary central incisors were the largest angle among the other teeth. However, our result was different from the studies of Kim et al. (2011) and Wang et al. (2014) which reported the greatest angulation was found in canines (16, 45), and



the study of Jung et al. (2017) which the maxillary lateral incisor was greater angulation than that of the maxillary central incisor (49). The reason for the differences caused by different methods and reference point of measurement. In our study, the sagittal angulation was measured from the alveolar bone axis and the tooth root axis which was a connecting line from midpoint of the cervical line to the apex of root. On the other hand, the other studies used the alveolar bone axis and the whole tooth axis as a reference line which was a line connecting from the incisal edge to the root apex (16, 45, 49) (Table 11).

**Table 11** Data of the previous studies and the present report of the root angulation of the maxillary anterior teeth within the alveolar bone

	Our study	Kim 2011	Wang 2014	Jung 2017
Central incisors	16.59° ± 5.97°	17.3° ± 14.1°	15.7° ± 6.1°	6.1° ± 3.9°
Lateral incisors	13.89 ± 6.12	16.1 ± 12.2	20.2 ± 7.9	12.1 ± 4.2
Canines	14.93° ± 6.02°	17.9° ± 6.2°	27.4° ± 8.7°	-
First premolars	13.38° ± 6.46°	-	20.0° ± 7.2°	-
<b>Definition of root axis</b>	A line connecting from the midpoint of the cervical line to the root apex	A line connecting from the incisal edge to the root apex	A line connecting from the incisal edge to the root apex	A line connecting from the lowest point of the crown to the highest point of the apex

The result of our study showed a moderate level of correlation between the right and left side of the anterior alveolar arch forms. The angulation between the dental root axis and the alveolar bone axis was also correlated in the same manner. Thereby, the position and axis of an implant in the anterior maxillary region could be guided by the angulation of the contralateral tooth root axis and the alveolar bone axis. Adjunctive bone augmentation may be required to build an appropriate contour of the anterior alveolar arch (63, 64).

While assessing the relationship between the root-to-bone angulation and the different anterior alveolar arch forms, the results demonstrated that the angulation between the tooth root axis and the alveolar bone axis was largely influenced by the intercanine depth. The intercanine depth represented as anterior arch depth. The angulation of the tooth root axis and alveolar bone axis decreased with a reduced intercanine depth of the alveolar arch. Thus, the long anterior alveolar arch form had a greater angulation between the root axis and the alveolar bone axis than the short anterior alveolar arch form. Moreover, the type of anterior alveolar arch form could be used to predict the angulation of the tooth root axis and the alveolar bone axis as shown in the equation.

The class I SRP had the greatest angulation between the dental root axis and the alveolar bone axis and provided a greater palatal bone thickness in comparison to the other classes.<sup>24</sup> Most of the maxillary teeth in the anterior esthetic zone in this study were classified as the Class I sagittal root position, while the Class III sagittal root

position was not found within the dataset used. This result is consistent with the findings of previous studies<sup>14, 21, 25-27</sup>. The frequencies of the Class III sagittal root position varied from 0.2 to 1.8%, indicating the rarity of this class of sagittal root position<sup>14, 21, 25-27</sup>. Therefore, palatal implant engagement in the anterior maxilla is recommended due to its sufficient palatal bone support, which affects proper primary implant stability during the immediate implant placement. Consequently, immediate implant placement is typically performed in the anterior esthetic region.

The classifications of the maxillary anterior teeth at mid-root position were categorized by several authors (15, 46-48). Each author classified the root position inside the alveolar bone with different classification criteria. Briefly, they classified the root position in the alveolar bone as buccal, middle, and palatal. Thus, the results were slightly different in some issues. Even though, our study used the classification of the root position reported by Kan et al. (2011) (15) and the overall frequency of the middle-type of the root position (sagittal root position class II and IV) was similar, our finding found a higher frequency of sagittal root position class II and a lower frequency of sagittal root position class IV, compared to the study of Kan et al. (2011) (Table 12). Lombardo et al. (2015) reported that The dental and alveolar arch forms were different in both width and depth in different ethnic groups (65). Therefore, the reason of this issue might be due to ethnic differences between Western and Eastern ethnic groups.

Table 12 Data of the Kan's study and the present study of the frequency distribution of the root position of the anterior maxillary teeth in the alveolar bone

	Kan 2011		Present study	
	Count	%	Count	%
Class I	487	81.1	667	85.1
Class II	39	6.5	82	10.5
Class III	4	0.7	-	-
Class IV	70	11.7	35	4.5
Overall	600	100	784	100

Most roots of the maxillary teeth in the anterior esthetic zone were located buccally within the alveolar bone (sagittal root position class I). This result was consistent with the results of previous studies (15, 46-49). The sagittal root position class I showed the greatest angulation between the dental root axis and the alveolar bone axis and provided greater palatal bone thickness in comparison to the other classes. Therefore, palatal implant engagement in the anterior maxilla is recommended due to its sufficient palatal bone support which affects proper primary implant stability during the immediate implant placement and the existing labial bone thickness at least 2 mm could be provided to reduce risk of labial bone

resorption, bone dehiscence and fenestration (1, 66, 67). Consequently, immediate implant placement is typically performed in the anterior esthetic region.

On the other hand, the root positioning more palatally inside the alveolar bone (sagittal root position class III) was not found within the dataset used. The frequency of the Class III sagittal root position varied from 0.2 to 1.8%, indicating the rarity of this class of sagittal root position (15, 46-49) (Table 13). Due to the root engaging the palatal cortical bone, the dental implant stability would rely on the existing labial bone. Tian et al. (2015) reported that palatal-type roots of the maxillary incisors (sagittal root position class III) had thinner labial supporting bone than the other classes (66). As a result, clinician should manage patients with sagittal root position class III carefully in order to prevent gingival recession, labial bone loss, fenestration and perforation (68).

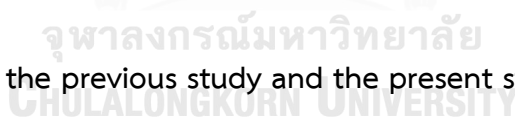


**Table 13** Data of the previous study and the present study of the frequency distribution of the palatal root position of the anterior maxillary teeth in the alveolar bone

	Palatal	
	Count	%
Kan 2011	4	0.7
Lau 2011	3	1.8

Chung 2014	1	0.4
Xu 2016	2	0.2
Jung 2017	2	0.25
Present study	0	0

The angulations between the root axis and the alveolar bone axis showed statistically significant differences from the classifications of both the sagittal root position and anterior alveolar arch form. From our study, the anterior alveolar arch shapes and types of sagittal root position explained the changes in root-to-bone angulation of approximately 2.5% and 9.5%, respectively. Moreover, the anterior alveolar arch form together with the sagittal root position influenced the variation of root-to-bone angulation approximately 11.7%. Based on our results shown in Table 5, the overall average root-to-bone angulation was smallest in short medium arch regardless of the SRP classification. When the arch depth increased, the overall average root-to-bone angulation increased, especially in the long medium arch.

Clinically, the alveolar arch form classification would be helpful during the selection of implant size when determining the number of implants and predicting bone augmentation because for long wide arches with a greater transversal width than the others, a larger implant diameter could be selected. In contrast, the SRP classification provided information for implant treatment planning not only for the

prevention of gingival recession, bone dehiscence and fenestration but also the selection of implant abutment types and the prosthetic design. As the drilling access point can assume the access hole of the implant abutment<sup>25</sup>, palatal implantation is suitable for the site with a class I SRP due to the thicker palatal native bone. The implant should be placed to mimic the original root angulation but located more palatally within the alveolar bone. As a result, a screw-retained restoration is suggested. In the case of sites with class II and IV SRP, where the volume of the labial and palatal bone was reduced, the dental implant should be placed to mimic the original root position and angulation. Consequently, longer implants and cement-retained restorations are recommended.

During implant treatment planning, the three-dimensional position and the angulation of implant was planned. Without any references, it is difficult to control the location of the drilling access and the angulation of the handpiece. Thus, the surgical guide is recommended to transfer the implant treatment plan to the implant placement site. The drilling access point can be assumed the access hole of implant abutment. These affect the selection of implant abutment types and the prosthetic design.

According to the present concept (69, 70), the implant placement is driven by restoration, meaning that the implant should be placed in a way which mimics the dental root axis. Since the sagittal root position class I is the most common, the thinned alveolar bone, especially in the labial aspect, tended to increase the risk of

bone perforation and bone cracking during osteotomy (71). This research recommends the use of a CBCT assessment as a standard method for presurgical evaluation of the implant site for determining the surrounding vital structure, the quality and volume of the existing bone. To minimize the recession of the labial bone and soft tissue, some authors recommended a minimum labial bone thickness of 1-2 mm (72, 73). As a result, while seeking to achieve long-term maintenance of both the esthetic result and function, surgeons should use a modified 3-dimensional implant position and angulation by placing a properly sized and shaped implant fixture slightly on the palatal side, and also fill the labial gap using bone grafting material during the immediate implant placement to ensure sufficient facial bone thickness. In addition, in case of insufficient bone volume, bone augmentation might be performed either during, or prior to implant placement (74, 75).

In summary, the angulation of the dental root axis and the alveolar bone axis plays important roles in determining implant position among the different anterior alveolar arch forms, and between the different classifications of the sagittal root position. Implant surgeons should be aware and use this information when determining where implants should be properly placed so that they can achieve a suitable result.



## REFERENCES

1. Buser D, Martin W, Belser UC. Optimizing esthetics for implant restorations in the anterior maxilla: anatomic and surgical considerations. *Int J Oral Maxillofac Implants*. 2004;19 Suppl:43-61.
2. Januario AL, Duarte WR, Barriviera M, Mesti JC, Araujo MG, Lindhe J. Dimension of the facial bone wall in the anterior maxilla: a cone-beam computed tomography study. *Clin Oral Implants Res*. 2011;22(10):1168-71.
3. Johnson K. A study of the dimensional changes occurring in the maxilla following tooth extraction. *Aust Dent J*. 1969;14(4):241-4.
4. Misch CE. Anterior Single-Tooth Replacement: Surgical Considerations. In: Misch CE, editor. third edition ed. Canada: Mosby Elsevier; 2008.
5. Moy PK, Pozzi A, Beumer III J. Surgical Considerations for the Esthetic zone. In: Beumer J, Faulkner RF, Shah K, Moy PK, editors. *Fundamentals of implant dentistry: Surgical principles*. 2. China: Quintessence Publishing; 2016. p. 291-332.
6. Jahangiri L, Devlin H, Ting K, Nishimura I. Current perspectives in residual ridge remodeling and its clinical implications: a review. *J Prosthet Dent*. 1998;80(2):224-37.
7. Van der Weijden F, Dell'Acqua F, Slot DE. Alveolar bone dimensional changes of post-extraction sockets in humans: a systematic review. *J Clin Periodontol*. 2009;36(12):1048-58.
8. Ferrario VF, Sforza C, Miani A, Jr., Tartaglia G. Mathematical definition of the shape of dental arches in human permanent healthy dentitions. *Eur J Orthod*. 1994;16(4):287-94.
9. Preti G, Pera P, Bassi F. Prediction of the shape and size of the maxillary anterior arch in edentulous patients. *J Oral Rehabil*. 1986;13(2):115-25.
10. Sagat G, Yalcin S, Gultekin BA, Mijiritsky E. Influence of arch shape and implant position on stress distribution around implants supporting fixed full-arch prosthesis in edentulous maxilla. *Implant Dent*. 2010;19(6):498-508.
11. Pietrokovski J, Starinsky R, Arensburg B, Kaffe I. Morphologic characteristics of bony edentulous jaws. *J Prosthodont*. 2007;16(2):141-7.

12. Bulyalert A, Pimkhaokham A. Arch form and alveolar bone thickness in maxillary anterior esthetic region: A cone beam computed tomography assessment. Thailand: Chulalongkorn University; 2015.
13. Suk KE, Park JH, Bayome M, Nam YO, Sameshima GT, Kook YA. Comparison between dental and basal arch forms in normal occlusion and Class III malocclusions utilizing cone-beam computed tomography. *Korean J Orthod.* 2013;43(1):15-22.
14. Bulyalert A, Pimkhaokham A. A novel classification of anterior alveolar arch forms and alveolar bone thickness: A cone beam computed tomography study. *Imaging Sci Dent.* 2018;48(3):191-9.
15. Kan JY, Roe P, Rungcharassaeng K, Patel RD, Waki T, Lozada JL, et al. Classification of sagittal root position in relation to the anterior maxillary osseous housing for immediate implant placement: a cone beam computed tomography study. *Int J Oral Maxillofac Implants.* 2011;26(4):873-6.
16. Wang HM, Shen JW, Yu MF, Chen XY, Jiang QH, He FM. Analysis of facial bone wall dimensions and sagittal root position in the maxillary esthetic zone: a retrospective study using cone beam computed tomography. *Int J Oral Maxillofac Implants.* 2014;29(5):1123-9.
17. Zhang S, Shi X, Liu H. Angulations of Anterior Teeth With Reference to the Alveolar Bone Measured by CBCT in a Chinese Population. *Implant Dent.* 2015;24(4):397-401.
18. Bryant RM, Sadowsky PL, Hazelrig JB. Variability in three morphologic features of the permanent maxillary central incisor. *Am J Orthod.* 1984;86(1):25-32.
19. Hair JFJ, Black WC, Babin BJ, Anderson RE, Tatham RL. *Multivariate Data Analysis.* USA: Pearson Education Inc.; 2006.
20. The glossary of prosthodontic terms. *J Prosthet Dent.* 2005;94:10-92.
21. Jivraj S, Chee W. Treatment planning of implants in the aesthetic zone. *Br Dent J.* 2006;201(2):77-89.
22. Pietrokovski J. The bony residual ridge in man. *J Prosthet Dent.* 1975;34(4):456-62.

23. Braun S, Hnat WP, Fender DE, Legan HL. The form of the human dental arch. *Angle Orthod.* 1998;68(1):29-36.
24. Sampson PD. Dental arch shape: a statistical analysis using conic sections. *Am J Orthod.* 1981;79(5):535-48.
25. Scott JH. The shape of the dental arches. *J Dent Res.* 1957;36(6):996-1003.
26. Bayome M, Park JH, Han SH, Baek SH, Sameshima GT, Kook YA. Evaluation of dental and basal arch forms using cone-beam CT and 3D virtual models of normal occlusion. *Aust Orthod J.* 2013;29(1):43-51.
27. Burris BG, Harris EF. Maxillary arch size and shape in American blacks and whites. *Angle Orthod.* 2000;70(4):297-302.
28. Papagiannis A, Halazonetis DJ. Shape variation and covariation of upper and lower dental arches of an orthodontic population. *Eur J Orthod.* 2016;38(2):202-11.
29. Moorrees CFA, Gron AM, Le Bret LM, Yen PK, FJ F. Growth studies of the dentition: A review. *Am J Orthod.* 1969;55(6):600-16.
30. Andrews L. The six elements of orofacial harmony. *Andrews J.* 2000;1:13-22.
31. Ball RL, Miner RM, Will LA, Arai K. Comparison of dental and apical base arch forms in Class II Division 1 and Class I malocclusions. *Am J Orthod Dentofacial Orthop.* 2010;138(1):41-50.
32. Uysal T, Memili B, Usumez S, Sari Z. Dental and alveolar arch widths in normal occlusion, class II division 1 and class II division 2. *Angle Orthod.* 2005;75(6):941-7.
33. Uysal T, Usumez S, Memili B, Sari Z. Dental and alveolar arch widths in normal occlusion and Class III malocclusion. *Angle Orthod.* 2005;75(5):809-13.
34. Bishara SE, Jakobsen JR, Treder J, Nowak A. Arch width changes from 6 weeks to 45 years of age. *Am J Orthod Dentofacial Orthop.* 1997;111(4):401-9.
35. Knott VB. Longitudinal study of dental arch widths at four stages of dentition. *Angle Orthod.* 1972;42(4):387-94.
36. Lee SJ, Lee S, Lim J, Park HJ, Wheeler TT. Method to classify dental arch forms. *Am J Orthod Dentofacial Orthop.* 2011;140(1):87-96.
37. Quimby M, Vig K, Rashid R, AR F.

The Accuracy and Reliability of Measurements Made on Computer-Based Digital Models. *Angle Orthod.* 2004;74:298-303.

38. Rheude B, Sadowsky P, Ferriera A, Jacobson A. An Evaluation of the Use of Digital Study Models in Orthodontic Diagnosis and Treatment Planning. *Angle Orthod.* 2005;75:300-4.

39. Stevens DR, Flores-Mir C, Nebbe B, Raboud DW, Heo G, Major PW. Validity, reliability, and reproducibility of plaster vs digital study models: comparison of peer assessment rating and Bolton analysis and their constituent measurements. *Am J Orthod Dentofacial Orthop.* 2006;129(6):794-803.

40. Cha BK, Lee YH, Lee NK, Choi DS, Baek SH. Soft tissue thickness for placement of an orthodontic miniscrew using an ultrasonic device. *Angle Orthod.* 2008;78(3):403-8.

41. Gupta D, Miner RM, Arai K, Will LA. Comparison of the mandibular dental and basal arch forms in adults and children with Class I and Class II malocclusions. *Am J Orthod Dentofacial Orthop.* 2010;138(1):10 e1-8; discussion -1.

42. Kim K, Bayome M, Kim K, Han SH, Kim Y, Baek SH, et al. Three-dimensional evaluation of the relationship between dental and basal arch forms in normal occlusion. *Korean J Orthod.* 2011;4:288-96.

43. Al-Ekrish AA, Ekram M. A comparative study of the accuracy and reliability of multidetector computed tomography and cone beam computed tomography in the assessment of dental implant site dimensions. *Dentomaxillofac Radiol.* 2011;40(2):67-75.

44. Baumgaertel S, Palomo JM, Palomo L, Hans MG. Reliability and accuracy of cone-beam computed tomography dental measurements. *Am J Orthod Dentofacial Orthop.* 2009;136(1):19-25; discussion -8.

45. Kim JH, Lee JG, Han DH, Kim HJ. Morphometric analysis of the anterior region of the maxillary bone for immediate implant placement using micro-CT. *Clin Anat.* 2011;24(4):462-8.

46. Lau SL, Chow J, Li W, Chow LK. Classification of maxillary central incisors-implications for immediate implant in the esthetic zone. *J Oral Maxillofac Surg.* 2011;69(1):142-53.

47. Chung SH, Park YS, Chung SH, Shon WJ. Determination of implant position for immediate implant placement in maxillary central incisors using palatal soft tissue landmarks. *Int J Oral Maxillofac Implants*. 2014;29(3):627-33.
48. Xu D, Wang Z, Sun L, Lin Z, Wan L, Li Y, et al. Classification of the Root Position of the Maxillary Central Incisors and its Clinical Significance in Immediate Implant Placement. *Implant Dent*. 2016;25(4):520-4.
49. Jung YH, Cho BH, Hwang JJ. Analysis of the root position of the maxillary incisors in the alveolar bone using cone-beam computed tomography. *Imaging Sci Dent*. 2017;47(3):181-7.
50. Mozzo P, Procacci C, Tacconi A, Martini PT, Andreis IA. A new volumetric CT machine for dental imaging based on the cone-beam technique: preliminary results. *Eur Radiol*. 1998;8(9):1558-64.
51. D'Addazio PS, Carvalho AC, Campos CN, Devito KL, Ozcan M. Cone beam computed tomography in Endodontics. *Int Endod J*. 2016;49(3):311-2.
52. Parker JM, Mol A, Rivera EM, Tawil PZ. Cone-beam Computed Tomography Uses in Clinical Endodontics: Observer Variability in Detecting Periapical Lesions. *J Endod*. 2016.
53. Patel S, Horner K. The use of cone beam computed tomography in endodontics. *Int Endod J*. 2009;42(9):755-6.
54. Scarfe WC, Levin MD, Gane D, Farman AG. Use of cone beam computed tomography in endodontics. *Int J Dent*. 2009;2009:634567.
55. Holberg C, Steinhäuser S, Geis P, Rudzki-Janson I. Cone-beam computed tomography in orthodontics: benefits and limitations. *J Orofac Orthop*. 2005;66(6):434-44.
56. Mamatha J, Chaitra KR, Paul RK, George M, Anitha J, Khanna B. Cone Beam Computed Tomography-Dawn of A New Imaging Modality in Orthodontics. *J Int Oral Health*. 2015;7(Suppl 1):96-9.
57. Nervina JM. Cone beam computed tomography use in orthodontics. *Aust Dent J*. 2012;57 Suppl 1:95-102.

58. Ahmad M, Jenny J, Downie M. Application of cone beam computed tomography in oral and maxillofacial surgery. *Aust Dent J.* 2012;57 Suppl 1:82-94.
59. Pohlenz P, Blessmann M, Blake F, Heinrich S, Schmelzle R, Heiland M. Clinical indications and perspectives for intraoperative cone-beam computed tomography in oral and maxillofacial surgery. *Oral Surg Oral Med Oral Pathol Oral Radiol Endod.* 2007;103(3):412-7.
60. Schwarz MS, Rothman SL, Chafetz N, Rhodes M. Computed tomography in dental implantation surgery. *Dent Clin North Am.* 1989;33(4):555-97.
61. Guerrero ME, Jacobs R, Loubele M, Schutyser F, Suetens P, van Steenberghe D. State-of-the-art on cone beam CT imaging for preoperative planning of implant placement. *Clin Oral Investig.* 2006;10(1):1-7.
62. Ronay V, Miner RM, Will LA, Arai K. Mandibular arch form: the relationship between dental and basal anatomy. *Am J Orthod Dentofacial Orthop.* 2008;134(3):430-8.
63. Buser D, Chen ST, Weber HP, Belser UC. Early implant placement following single-tooth extraction in the esthetic zone: biologic rationale and surgical procedures. *Int J Periodontics Restorative Dent.* 2008;28(5):441-51.
64. Huynh-Ba G, Pjetursson BE, Sanz M, Cecchinato D, Ferrus J, Lindhe J, et al. Analysis of the socket bone wall dimensions in the upper maxilla in relation to immediate implant placement. *Clin Oral Implants Res.* 2010;21(1):37-42.
65. Lombardo L, Coppola P, Siciliani G. Comparison of dental and alveolar arch forms between different ethnic groups. *Int Orthod.* 2015;13(4):462-88.
66. Tian YL, Liu F, Sun HJ, Lv P, Cao YM, Yu M, et al. Alveolar bone thickness around maxillary central incisors of different inclination assessed with cone-beam computed tomography. *Korean J Orthod.* 2015;45(5):245-52.
67. Spray JR, Black CG, Morris HF, Ochi S. The influence of bone thickness on facial marginal bone response: stage 1 placement through stage 2 uncovering. *Ann Periodontol.* 2000;5(1):119-28.
68. Sung CE, Cochran DL, Cheng WC, Mau LP, Huang PH, Fan WH, et al. Preoperative assessment of labial bone perforation for virtual immediate implant surgery in the

maxillary esthetic zone: A computer simulation study. *J Am Dent Assoc.* 2015;146(11):808-19.

69. Garber DA. The esthetic dental implant: letting restoration be the guide. *J Am Dent Assoc.* 1995;126(3):319-25.

70. Garber DA, Belser UC. Restoration-driven implant placement with restoration-generated site development. *Compend Contin Educ Dent.* 1995;16(8):796, 8-802, 4.

71. Braut V, Bornstein MM, Belser U, Buser D. Thickness of the anterior maxillary facial bone wall-a retrospective radiographic study using cone beam computed tomography. *Int J Periodontics Restorative Dent.* 2011;31(2):125-31.

72. Cho YB, Moon SJ, Chung CH, Kim HJ. Resorption of labial bone in maxillary anterior implant. *J Adv Prosthodont.* 2011;3(2):85-9.

73. Grunder U, Gracis S, Capelli M. Influence of the 3-D bone-to-implant relationship on esthetics. *Int J Periodontics Restorative Dent.* 2005;25(2):113-9.

74. Araujo MG, Linder E, Lindhe J. Bio-Oss collagen in the buccal gap at immediate implants: a 6-month study in the dog. *Clin Oral Implants Res.* 2011;22(1):1-8.

75. Mehta H, Shah S. Management of Buccal Gap and Resorption of Buccal Plate in Immediate Implant Placement: A Clinical Case Report. *J Int Oral Health.* 2015;7(Suppl 1):72-5.

## APPENDIX

Data of anterior alveolar arch form  
classification

Case No.	Arch type
1	3
2	3
3	2
4	4
5	3
6	3
7	3
8	4
9	2
10	4
11	2
12	4
13	4
14	3
15	4

Case No.	Arch type
16	3
17	2
18	1
19	2
20	4
21	1
22	4
23	3
24	1
25	2
26	1
27	4
28	3
29	1
30	3
31	3
32	1
33	1
34	1



Case No.	Arch type
35	2
36	4
37	1
38	1
39	3
40	4
41	3
42	1
43	1
44	4
45	4
46	3
47	1
48	2
49	1
50	1
51	3
52	3
53	4

Case No.	Arch type
54	3
55	3
56	3
57	3
58	1
59	1
60	1
61	1
62	3
63	3
64	3
65	3
66	1
67	3
68	4
69	4
70	1
71	1
72	4

Case No.	Arch type
73	1
74	3
75	3
76	4
77	1
78	1
79	3
80	3
81	3
82	2
83	4
84	1
85	4
86	2
87	1
88	1
89	1
90	4
91	1

Case No.	Arch type
92	2
93	4
94	4
95	2
96	4
97	4
98	4

#### Anterior arch form classification

Type 1: Long Narrow

Type 2: Short Medium

Type 3: Long Medium

Type 4: Long Wide

## Arch Type I: Long Narrow

Case no.	Angle #14	SRP #14	Angle #13	SRP #13	Angle #12	SRP #12	Angle #11	SRP #11	Angle #21	SRP #21	Angle #22	SRP #22	Angle #23	SRP #23	Angle #24	SRP #24
18	14.17	4	12.37	1	12.85	1	14.98	2	16.21	2	15.06	2	14.19	1	12.74	1
21	11.8	1	11.69	1	11.15	1	10.93	1	8.71	1	12.92	1	20.96	1	9.12	1
24	17.04	1	22.01	1	9.68	1	11.81	1	18.43	1	12.47	1	19.78	1	13.28	2
26	17.39	1	21.01	1	22.02	1	24.15	1	24.51	1	24.41	1	15.49	1	20.06	1
29	14.34	2	19.54	1	22.72	1	22.16	1	22.34	1	24.53	1	14.74	1	16.43	1
32	8.78	1	12.78	1	4.3	2	8.19	2	6.07	2	7.03	1	13.11	1	10.95	1
33	5.21	4	12.1	1	4.13	4	12.45	2	5.54	2	0.67	4	6.26	1	10.97	1
34	7.97	1	11.69	1	15.19	1	14.7	1	15.77	1	14.69	1	11.47	1	12.05	1
37	18.78	2	20.15	1	11.43	1	11.44	2	13.26	2	13.64	1	16.62	1	10.68	1
38	10.59	1	12.99	1	12.25	1	9.2	1	17.36	1	16.3	1	14.61	1	4.36	1
42	12.12	2	18.68	1	13.39	1	16.74	2	14.01	2	20.89	1	20.85	1	13.26	2
43	13.11	1	21.48	1	27.67	1	29.21	2	27.53	2	25.15	1	20.13	1	14.68	1
47	4.02	1	11.86	1	20.17	1	12.94	1	13.99	1	15.57	1	6.53	1	5.6	1
49	12.82	1	7.52	1	12.35	1	17.66	1	9.72	1	17.44	1	14.18	1	2.93	2
50	25.8	1	21.12	1	17.48	1	17.3	2	11.28	1	8.49	1	15.48	1	22.42	1
58	20.96	1	28.1	1	20.44	1	26.92	2	19.55	2	19.71	2	20.17	1	18.68	1
59	7.87	4	14.85	1	4.09	4	14.59	1	14.13	1	9.52	1	8.65	1	9.4	1
60	3.42	1	17.04	1	16.92	1	12.84	1	15.55	1	18.16	1	16.74	1	5.82	4

61	6.5	1	7.36	1	9.84	2	6.25	2	17.17	1	9.25	1	10.86	1	5.84	2
66	9.91	2	15.89	1	8.02	1	23.36	1	16.12	1	9.7	4	13.76	1	17.28	1
70	23.12	1	19.41	1	18.62	1	27.27	1	20.28	1	7.16	4	22.39	1	20.11	1
71	12.23	1	8.79	1	5.37	1	17.64	1	16.11	1	11.89	1	6.72	1	10.32	1
73	30.64	1	35.23	1	22.42	1	23.64	1	22.82	1	26.41	1	28.58	1	21.79	2
77	12.52	1	16.19	1	5.06	1	12.12	1	8.48	1	18.96	1	10.98	1	14.56	1
78	10.21	1	17.08	1	10.44	2	17.81	2	13.71	1	8.47	3	24.11	1	14.36	1
84	8.62	1	8.66	1	8.38	4	8.8	1	6.17	1	5.99	4	7.2	1	10.48	1
87	13.54	1	16.24	1	10.4	1	11.77	1	12.76	1	1.97	1	0.61	1	2.65	1
88	6.13	1	11.92	1	8.58	1	14.8	1	20.63	1	13.25	1	29.02	1	13.3	1
89	8.09	4	11.4	1	8.98	1	10.54	1	13.95	1	8.01	1	8.06	1	16.59	2
91	3.49	1	0.4	1	11.14	1	7.04	1	9	1	10.57	1	6.79	1	9.08	1

## Arch type II: Short Medium

Case no.	Angle #14	SRP #14	Angle #13	SRP #13	Angle #12	SRP #12	Angle #11	SRP #11	Angle #21	SRP #21	Angle #22	SRP #22	Angle #23	SRP #23	Angle #24	SRP #24
3	9.27	1	12.78	1	15.44	1	16.49	1	20.67	1	10.41	1	12.9	1	16.39	1
9	24.62	1	13.17	1	9.9	1	8.13	1	7.18	2	1.71	4	3.94	1	14.29	1
11	16.88	1	9.32	1	17.72	1	11.75	1	20.41	1	20.63	1	18.43	1	21.45	1
17	17.96	1	13.74	1	15.1	1	16.19	1	19.96	1	22.02	1	21.39	1	20.06	1
19	19.81	1	11.56	1	17.05	1	19.05	1	11.43	1	12.35	1	5.95	1	17.44	1
25	9.62	2	8.69	1	14.46	1	11.68	1	7.22	2	4.87	1	10.04	1	11.33	1
35	9.81	1	15.79	1	8.01	4	13.12	1	16.09	1	8.16	4	16.41	1	7.75	2
48	6.09	1	8.22	1	9.84	1	8.82	1	6.84	2	1.69	4	3.55	1	12.68	1
82	2.87	1	11.83	1	11.65	1	8.54	1	18.9	1	15.96	1	16.9	1	11.65	1
86	14.84	1	8.61	1	20.04	1	13.88	1	18.43	1	19.33	1	15.42	1	21.68	1
92	8.56	1	7.37	1	5.8	4	17.74	1	14.56	1	1.08	4	10.59	1	22.09	1
95	4.18	1	9.91	1	5.78	1	12.25	1	4.48	2	0.82	1	11.22	1	5.1	1

## Arch type III: Long Medium

Case no.	Angle #14	SRP #14	Angle #13	SRP #13	Angle #12	SRP #12	Angle #11	SRP #11	Angle #21	SRP #21	Angle #22	SRP #22	Angle #23	SRP #23	Angle #24	SRP #24
1	24.14	1	18.23	1	12.72	1	17.23	1	22.38	1	19.44	1	18.32	1	27.81	1
2	18.73	1	8.54	1	10.21	1	13.48	1	13.85	1	9.3	1	13.08	1	20.46	1
5	13.76	1	10.36	1	10.3	1	21.81	1	24.41	1	15.04	1	9.84	4	3.3	4
6	6.75	1	9.5	1	6.9	4	14.5	1	16	1	6.2	4	12.27	1	15.67	1
7	10.78	1	11.5	1	8.48	1	10.16	1	8.84	1	12.53	1	9.51	1	10.21	4
14	23.92	1	24.87	1	16.17	1	14.21	2	14.31	2	8.44	2	18.22	1	17.46	1
16	12.11	4	16.09	1	9.69	1	22.52	1	6.26	2	4.32	4	23.92	1	5.68	4
23	13.25	1	16.36	1	9.61	1	15.14	1	15.22	1	16.79	1	13.3	1	11.89	1
28	4.99	1	10.88	1	10.04	1	19.3	1	19.84	1	13.76	1	11.21	1	7.71	1
30	12.33	1	17.02	1	11.51	1	20.33	1	24.51	1	22.02	1	21.93	1	10.86	1
31	8.08	2	17.62	1	16.55	1	17.4	1	15.32	2	15.1	1	16.11	1	2.38	2
39	4.78	2	26.61	1	23.43	1	32.17	1	24.51	1	21.42	1	26.28	1	12.45	2
41	24.92	1	26.49	1	20.99	1	20.12	1	18.2	1	28.74	1	27.09	1	20.98	1
46	18.58	1	17.53	1	10.35	1	21.77	1	18.23	1	9.47	1	14.61	1	7.9	1
51	10.81	1	22.68	1	22.89	1	25.3	1	23.88	2	26.24	1	21.32	1	13.43	1
52	17.76	2	13.39	1	17.11	2	10.56	2	14.36	2	18.8	1	13.91	1	9.32	2
54	16.92	1	20.1	1	17.01	1	21.31	2	18.61	2	15.17	1	17.72	1	12.69	1
55	9.07	1	21.35	1	18.37	1	20.79	1	22.89	1	11.49	1	15.14	1	6.87	1

56	5.58	2	9.95	1	13.58	1	15.6	1	28.75	1	21.9	1	19.82	1	8.83	2
57	15.7	1	26.96	1	19	1	21.79	1	21.73	1	19.14	1	22.49	1	20.14	1
62	16.02	1	9.22	1	13.15	1	18.85	1	15.38	1	10.66	1	8.51	1	9.65	1
63	16.53	1	18.17	1	18.52	1	19.01	1	19.6	1	17.74	1	16.82	1	12.12	1
64	4.45	4	9.77	1	13.65	1	12.83	1	15.98	1	17.06	1	11.67	1	4.65	4
65	25.79	2	21.84	1	21.37	1	15.54	1	21.34	1	27.85	1	27.73	1	24.3	1
67	15.62	1	20.25	1	13.38	1	15.6	1	16.7	1	13.52	1	24.15	1	15.86	1
74	18.67	1	9.8	1	7.48	4	13.19	1	12.24	1	3.81	4	10.17	1	14.35	1
75	13.68	1	10.14	1	20.76	1	19.91	1	18.7	1	8.08	1	13.12	1	4.48	2
79	21.08	1	14.56	1	15.12	1	3.16	1	13.22	1	11.78	2	16.62	1	20.42	1
80	8.27	2	5.34	1	10.3	1	15.2	1	21.53	1	7.34	1	7.68	1	5.15	4
81	5.83	1	9.06	1	20.78	1	24.43	1	20.54	1	14.44	1	9.54	1	7.3	1

Type IV: Long Wide

Case no.	Angle #14	SRP #14	Angle #13	SRP #13	Angle #12	SRP #12	Angle #11	SRP #11	Angle #21	SRP #21	Angle #22	SRP #22	Angle #23	SRP #23	Angle #24	SRP #24
4	23.51	1	11.44	1	10.19	1	21.97	1	18.31	1	9.69	1	14.56	1	11.85	1
8	3.96	1	7.63	1	13.5	1	11.82	1	10.61	1	14.93	1	8.29	1	9.09	4
10	6.68	1	12.58	1	13.47	1	18.87	1	17.22	1	15.49	1	10.31	1	7.66	1
12	24.25	1	21.9	1	25.94	1	21.27	1	20.43	1	18.74	1	14.8	1	16.84	1
13	17.35	1	17.14	1	9.04	2	6.18	2	17.76	2	11.38	1	18.25	1	11.25	2
15	22.77	1	8.63	2	9.61	1	9.83	2	9.96	2	10.81	1	11.08	1	19.27	1
20	14.59	1	16.93	1	12.59	1	21.3	1	21.2	1	13.92	1	17.05	1	16.81	1
22	13.42	1	16.8	1	14.21	1	17.22	2	13.8	2	12.86	1	11.57	1	16.45	1
27	15.22	1	22.25	1	14.33	1	11.61	1	10.63	1	9.47	1	11	1	12.61	1
36	9.79	1	15.79	1	8.01	4	13.12	1	16.09	1	8.16	4	16.41	1	7.75	2
40	26.27	2	20.44	1	11.4	1	21.78	1	13.62	1	12.56	1	14.42	1	11.64	1
44	17.56	1	19.12	1	17.32	1	19.55	2	20.4	2	21.04	1	21.56	1	29.17	1
45	19.97	1	9.43	1	8.85	1	11.57	1	6.97	1	7.16	1	7.47	1	11.62	1
53	17.39	1	17.11	1	24.95	1	28.94	1	28.34	1	25.21	1	21.6	1	20.14	1
68	15.46	1	26.76	1	12.67	1	19.1	1	24.36	1	12.7	1	22.77	1	8.93	1
69	21.34	1	14.2	1	9.61	1	7.87	1	19.73	1	14.48	1	15.07	1	14.28	1
72	17.78	1	13.06	1	21.88	1	18.47	1	23.19	1	22.02	1	17.01	1	16.07	1
76	9.05	1	11.37	1	14.45	1	17.69	1	15.94	1	14.46	1	13.3	1	9.38	1



83	23.73	1	21.31	1	11.72	1	16.12	1	22.35	1	10.34	1	20.46	1	29.46	1
85	21.9	1	15.28	1	15.82	1	25.41	1	19.73	1	11.09	1	12.33	1	10.78	1
90	4.06	1	12.13	1	20.51	1	8.33	1	15.97	1	21.21	1	11.3	1	3.84	1
93	14.76	1	23.5	1	23.54	1	33.12	1	28.94	1	32.41	1	16.52	1	15.14	1
94	24.37	2	15.27	1	9.28	1	26.57	1	28.16	1	19.49	1	17.45	1	27.81	2
96	2.64	1	18.98	1	20.86	1	22.54	1	24.05	1	18.77	1	21.5	1	14.43	1
97	1.01	2	1.98	1	7.15	1	12.6	2	1.1	2	3.89	4	2.53	1	8.6	2
98	9.14	1	11.77	1	16.71	1	18.59	1	16.01	1	12.3	1	7.9	1	13.77	1



Statistical analysis

Independent samples T-test comparing the right and the left sides of the maxillary central incisors, lateral incisors, canines, and first premolars.

Group Statistics

	Tooth	N	Mean	Std. Deviation	Std. Error Mean
Angle	Tooth 14	98	13.50276	6.694833	.676280
	Tooth 24	98	13.17184	6.128577	.619080

Independent Samples Test

		Levene's Test for Equality of Variances		t-test for Equality of Means						
		F	Sig.	t	df	Sig. (2-tailed)	Mean Difference	Std. Error Difference	95% Confidence Interval of the Difference	
									Lower	Upper
Angle	Equal variances assumed	1.762	.186	.361	194	.719	.330918	.916850	-1.477356	2.139193
	Equal variances not assumed			.361	192.504	.719	.330918	.916850	-1.477444	2.139281

## Group Statistics

	h	h 13	h 23	Toot	N	Mean	Std. Deviation	Mean	Std. Error
ngle	A	h 13	h 23	Toot	98	15.04	6.030157	.609138	
				Toot	98	14.78	5.919855	.597996	

## Independent Samples Test

	Levene's Test for Equality of Variances		t-test for Equality of Means							
	F	Sig.	t	df	Sig. (2-tailed)	Mean Difference	Error Difference	Std. Error Difference	95% Confidence Interval of the Difference	
ngle	.079	.779	.3	94	.760	.26105	.85360	.85360	Lower	Upper
ngle			.3	93.934	.760	.26105	.85360	.85360	1.422494	1.9445
									-	1.9445
									1.422497	99

## Group Statistics

	Tooth	N	Mean	Std. Deviation	Std. Error Mean
Angle	Tooth 12	98	13.78551	5.364746	.541921
	Tooth 22	98	13.68490	6.662667	.673031

## Independent Samples Test

		Levene's Test for Equality of Variances		t-test for Equality of Means						
		F	Sig.	t	df	Sig. (2-tailed)	Mean Difference	Std. Error Difference	95% Confidence Interval of the Difference	
									Lower	Upper
Angle	Equal variances assumed	3.176	.076	.116	194	.907	.100612	.864089	-1.603602	1.804826
	Equal variances not assumed			.116	185.554	.907	.100612	.864089	-1.604089	1.805313

Group Statistics

	Tooth	N	Mean	Std. Deviation	Std. Error Mean
Angle	Tooth 11	98	16.50765	6.052762	.611421
	Tooth 21	98	16.53378	5.939036	.599933



Independent Samples Test

		Levene's Test for Equality of Variances			t-test for Equality of Means					
		F	Sig.	t	df	Sig. (2-tailed)	Mean Difference	Std. Error Difference	95% Confidence Interval of the Difference	
									Lower	Upper
Angle	Equal variances assumed	.168	.682	-.030	194	.976	-.026122	.856596	-1.715558	1.663313
	Equal variances not assumed			-.030	193.930	.976	-.026122	.856596	-1.715562	1.663317

Correlation coefficient (r) from Pearson correlation analysis between the right and the left sides.

Correlations

		Right	Left
Right	Pearson Correlation	1	.657**
	Sig. (2-tailed)		.000
	N	392	392
Left	Pearson Correlation	.657**	1
	Sig. (2-tailed)	.000	
	N	392	392

\*\* . Correlation is significant at the 0.01 level (2-tailed).



## VITA

NAME Suweera Petaibunlue, DDS

DATE OF BIRTH 26 November 1987

PLACE OF BIRTH Songkhla, Thailand

INSTITUTIONS ATTENDED Preceptorship Program in Advanced Prosthodontics from  
University of California, Los Angeles School of Dentistry,  
California, USA

HOME ADDRESS 1525/214 Phaholyothin Road, Phaya Thai, Phaya Thai,  
Bangkok, 10400, Thailand

